REPORT DOCUMENTATION PAGE

Form Approved
OMB No. 0704-0188

1. AGENCY USE ONLY *(Leave blank)*	2. REPORT DATE	3. REPORT TYPE AND DATES COVERED
	1996	

4. TITLE AND SUBTITLE
Flutter Analysis and Analytic Sensitivities For Trapezoidal Panels

5. FUNDING NUMBERS

6. AUTHOR(S)

David Mineau

7. PERFORMING ORGANIZATION NAME(S) AND ADDRESS(ES)
AFIT Student Attending:
University of Washington

8. PERFORMING ORGANIZATION REPORT NUMBER
96-004

9. SPONSORING/MONITORING AGENCY NAME(S) AND ADDRESS(ES)
DEPARTMENT OF THE AIR FORCE
AFIT/CI
2950 P STREET, BLDG 125
WRIGHT-PATTERSON AFB OH 45433-7765

10. SPONSORING/MONITORING AGENCY REPORT NUMBER

11. SUPPLEMENTARY NOTES

12a. DISTRIBUTION/AVAILABILITY STATEMENT
Approved for Public Release IAW AFR 190-1
Distribution Unlimited
BRIAN D. GAUTHIER, MSgt, USAF
Chief Administration

12b. DISTRIBUTION CODE

13. ABSTRACT *(Maximum 200 words)*

19960531 103

14. SUBJECT TERMS	15. NUMBER OF PAGES
	79
	16. PRICE CODE

17. SECURITY CLASSIFICATION OF REPORT	18. SECURITY CLASSIFICATION OF THIS PAGE	19. SECURITY CLASSIFICATION OF ABSTRACT	20. LIMITATION OF ABSTRACT

NSN 7540-01-280-5500

Standard Form 298 (Rev. 2-89)
Prescribed by ANSI Std. Z39-18
298-102

GENERAL INSTRUCTIONS FOR COMPLETING SF 298

The Report Documentation Page (RDP) is used in announcing and cataloging reports. It is important that this information be consistent with the rest of the report, particularly the cover and title page. Instructions for filling in each block of the form follow. It is important to ***stay within the lines*** to meet ***optical scanning requirements***.

Block 1. Agency Use Only *(Leave blank)*.

Block 2. Report Date. Full publication date including day, month, and year, if available (e.g. 1 Jan 88). Must cite at least the year.

Block 3. Type of Report and Dates Covered. State whether report is interim, final, etc. If applicable, enter inclusive report dates (e.g. 10 Jun 87 - 30 Jun 88).

Block 4. Title and Subtitle. A title is taken from the part of the report that provides the most meaningful and complete information. When a report is prepared in more than one volume, repeat the primary title, add volume number, and include subtitle for the specific volume. On classified documents enter the title classification in parentheses.

Block 5. Funding Numbers. To include contract and grant numbers; may include program element number(s), project number(s), task number(s), and work unit number(s). Use the following labels:

C	Contract	PR	Project
G	Grant	TA	Task
PE	Program Element	WU	Work Unit Accession No.

Block 6. Author(s). Name(s) of person(s) responsible for writing the report, performing the research, or credited with the content of the report. If editor or compiler, this should follow the name(s).

Block 7. Performing Organization Name(s) and Address(es). Self-explanatory.

Block 8. Performing Organization Report Number. Enter the unique alphanumeric report number(s) assigned by the organization performing the report.

Block 9. Sponsoring/Monitoring Agency Name(s) and Address(es). Self-explanatory.

Block 10. Sponsoring/Monitoring Agency Report Number. *(If known)*

Block 11. Supplementary Notes. Enter information not included elsewhere such as: Prepared in cooperation with...; Trans. of...; To be published in.... When a report is revised, include a statement whether the new report supersedes or supplements the older report.

Block 12a. Distribution/Availability Statement. Denotes public availability or limitations. Cite any availability to the public. Enter additional limitations or special markings in all capitals (e.g. NOFORN, REL, ITAR).

- **DOD** - See DoDD 5230.24, "Distribution Statements on Technical Documents."
- **DOE** - See authorities.
- **NASA** - See Handbook NHB 2200.2.
- **NTIS** - Leave blank.

Block 12b. Distribution Code.

- **DOD** - Leave blank.
- **DOE** - Enter DOE distribution categories from the Standard Distribution for Unclassified Scientific and Technical Reports.
- **NASA** - Leave blank.
- **NTIS** - Leave blank.

Block 13. Abstract. Include a brief *(Maximum 200 words)* factual summary of the most significant information contained in the report.

Block 14. Subject Terms. Keywords or phrases identifying major subjects in the report.

Block 15. Number of Pages. Enter the total number of pages.

Block 16. Price Code. Enter appropriate price code *(NTIS only)*.

Blocks 17. - 19. Security Classifications. Self-explanatory. Enter U.S. Security Classification in accordance with U.S. Security Regulations (i.e., UNCLASSIFIED). If form contains classified information, stamp classification on the top and bottom of the page.

Block 20. Limitation of Abstract. This block must be completed to assign a limitation to the abstract. Enter either UL (unlimited) or SAR (same as report). An entry in this block is necessary if the abstract is to be limited. If blank, the abstract is assumed to be unlimited.

★U.S.GPO:1990-0-273-271

FLUTTER ANALYSIS AND ANALYTIC SENSITIVITIES FOR TRAPEZOIDAL PANELS

by

David Mineau

2nd Lieutenant, USAF

Abstract

Explicit expressions for the stiffness, geometric stiffness, mass, and aerodynamic force matrices are derived for the flutter analysis of simply supported composite wing panels. The formulation is based on Ritz analysis using simple polynomials and Piston Theory aerodynamics. The use of simple polynomials eliminates the need for numerical quadrature and decreases computation time. Analytic sensitivities of the aeroelastic system matrices and critical dynamic pressures are obtained with respect to layer thickness, fiber direction, and panel shape. The method is integrated with wing box analysis based on either the equivalent plate approach or finite element method, making it possible to obtain sensitivities of the stability boundary with respect to wing planform shape or locations of ribs and spars. The analytic sensitivities are used to construct approximations of the aeroelastic stability boundary for integrated wing / panel design synthesis.

ABBREVIATED BIBLIOGRAPHY

1. Dowell, E.H., Aeroelasticity of Plates and Shells, Noordhoff International Publishers, Leyden, 1975.

2. Sander, G., Bon, C., and Geradin, M., "Finite Element Analysis of Supersonic Panel Flutter", Internation Journal for Numerical Methods in Engineering, 7, pp. 379-394, 1973.

3. Bismarck-Nasr, M.,N., "Finite Element Analysis of Aeroelasticity of Plates and Shells", ASME Applied Mechanics Reviews, Vol. 45, No. 12, pp. 461-482, December 1992.

4. Hajela, P., and Glowasky, R., "Application of Piezoelectric Elements in Supersonic Panel Flutter Suppression", AIAA Paper 91-3191, AIAA Aircraft Design Systems and Operations Meeting, Baltimore, MD, September 1991.

5. Scott, R.C., and Weishaar, T.A., "Controlling Panel Flutter Using Adaptive Materials", AIAA Paper 91-1007, April 1991.

6. Dowell, E.H., and Ilgamov, M., Studies in Nonlinear Aeroelasticity, Springer-Verlag, New York, 1988.

7. Frampton, K.D., Clark, R.L., and Dowell, E.H., "State Space Modeling for Aeroelastic Panels Subject to Linearized Potential Flow Aerodynamic Loading", AIAA Paper 95-1294, Proceedings of the 36th AIAA/ASME/ASCE/AHS/ASC Structures, Structural Dynamics, and Materials Conference, New Orleans, LA, April 10-13, 1995, Vol. 2, pp. 1183-1189.

8. Kariappa, Somashekar, B.R., and Shah, C.G., "Discrete Element Approach to Flutter of Skew Panels with IN-Plane Forces Under Yawed Supersonic Flow", AIAA Journal, Vol. 8, No. 11, November 1970, pp. 2017-2022.

9. Chowdary, T.V.R., Sinha, P.K., and Parthan, S., "Finite Element Flutter Analysis of Composite Skew Panels", Computers & Structures, Vol. 58, No. 3, pp. 613-620, 1996.

10. Voss, H. M., and Dowell, E. H., "Effect of Aerodynamic Damping on Flutter of Thin Panels", AIAA Journal, Vol. 2, No. 1, January 1964, pp119-120.

11. Lottatti, I., "The Role of Damping on Supersonic Panel Flutter", AIAA Journal, Vol. 23, No. 10, October 1985, pp. 1640-1642.

12. Giles, G.L., "Equivalent Plate Analysis of Aircraft Wing Box Structures with General Planform Geometry", Journal of Aircraft, Vol. 23, No. 11, November 1986, pp. 859-864.

13. Giles, G.L., "Further Generalization of an Equivalent Plate Representation for Aircraft Structural Analysis", Journal of Aircraft, Vol. 26, No. 1, January 1989, pp. 67-74.

14. Livne, E., "Integrated Multidisciplinary Optimization of Actively Controlled Fiber Composite Wings", Ph.D. dissertation, Mechanical, Aerospace and Nuclear Engineering Department, University of California, Los Angeles, 1990.

15. Livne, E., "Analytical Sensitivities for Shape Optimization in Equivalent Plate Structural Wing Models", Journal of Aircraft, Vol. 31, No. 4, pp. 961-969, July-August 1994.

16. Livne, E., and Li, W-L., "Aeroservoelastic Aspects of Wing / Control Surface Planform Shape Optimization", AIAA Journal, Vol. 33, No. 2, February 1995, pp. 302-311.

17. Livne, E., and Milosavljevic, R., "Analytic Sensitivity and Approximation of Skin Buckling Constraints in Wing Shape Synthesis", Journal of Aircraft, Vol. 32, No. 5, September-October 1995, pp. 1102-1113.

18. Li, W-L., and Livne, E., "Analytic Sensitivities and Approximations in Supersonic and Subsonic Wing / Control Surface Unsteady Aerodynamics", AIAA Paper 95-1219, AIAA/ASME/ASCE/AHS/ASC 36th Structures, Structural Dynamics and Materials Conference, New Orleans, April 1995.

19. Haftka, R.T., and Gurdal, Z., "Elements of Structural Optimization", Third Edition, Kluwer Academic Publishers, Dordrecht, Boston, London 1991. (Chapter 6)

20. Pedersen, P., and Seyranian, A., "Sensitivity Analysis for Problems of Dynamic Stability", International Journal of Solids and Structures, Vol. 19, No. 4, pp. 315-335, 1983.

21. Seyranian, A., "Sensitivity Analysis of Multiple Eigenvalues", Mechanical Structures and Machines, Vol. 21, No. 2, pp. 261-284, 1993.

22. Golub, G., and Van Loan, C. F., Matrix Computations, 2nd edition, Johns Hopkins University Press, 1989.

23. Lecina, G., and Petiau, C., "Advances in Optimal Design with Composite Materials", in Computer Aided Optimal Design: Structuyral and Mechanical Systems, C.A. Mota Soares, editor, Springer Verlag, Berlin, 1987, pp. 943-953.

24. Ausman, J.D., Hangen, J.A., and Acevedo, D.A., "Application of a Local Panel Buckling Constraint within Automated Multidisciplinary Structural Analysis and Design", AIAA 92-1116, 1992 Aerospace Design Conference, February 3-6, 1992, Irvine, CA.

25. Bruhn, E.F., Analysis and Design of Flight Vehicle Structures, Tri State Offset Company, 1973, Chapter C5.

26. Whitney, J. M., Structural Analysis of Laminated Anisotropic Plates, Technomic Publishing Company, Lancaster, PA, 1987.

27. Tsai, S.W., and Hahn, H.T., Introduction to Composite Materials, Technomic Publishing Company, Lancaster, PA, 1980.

FLUTTER ANALYSIS AND ANALYTIC SENSITIVITIES FOR TRAPEZOIDAL PANELS

by

David Mineau

2nd Lieutenant, USAF

Abstract

Explicit expressions for the stiffness, geometric stiffness, mass, and aerodynamic force matrices are derived for the flutter analysis of simply supported composite wing panels. The formulation is based on Ritz analysis using simple polynomials and Piston Theory aerodynamics. The use of simple polynomials eliminates the need for numerical quadrature and decreases computation time. Analytic sensitivities of the aeroelastic system matrices and critical dynamic pressures are obtained with respect to layer thickness, fiber direction, and panel shape. The method is integrated with wing box analysis based on either the equivalent plate approach or finite element method, making it possible to obtain sensitivities of the stability boundary with respect to wing planform shape or locations of ribs and spars. The analytic sensitivities are used to construct approximations of the aeroelastic stability boundary for integrated wing / panel design synthesis.

ABBREVIATED BIBLIOGRAPHY

1. Dowell, E.H., Aeroelasticity of Plates and Shells, Noordhoff International Publishers, Leyden, 1975.

2. Sander, G., Bon, C., and Geradin, M., "Finite Element Analysis of Supersonic Panel Flutter", Internation Journal for Numerical Methods in Engineering, 7, pp. 379-394, 1973.

3. Bismarck-Nasr, M.,N., "Finite Element Analysis of Aeroelasticity of Plates and Shells", ASME Applied Mechanics Reviews, Vol. 45, No. 12, pp. 461-482, December 1992.

4. Hajela, P., and Glowasky, R., "Application of Piezoelectric Elements in Supersonic Panel Flutter Suppression", AIAA Paper 91-3191, AIAA Aircraft Design Systems and Operations Meeting, Baltimore, MD, September 1991.

5. Scott, R.C., and Weishaar, T.A., "Controlling Panel Flutter Using Adaptive Materials", AIAA Paper 91-1007, April 1991.

6. Dowell, E.H., and Ilgamov, M., Studies in Nonlinear Aeroelasticity, Springer-Verlag, New York, 1988.

7. Frampton, K.D., Clark, R.L., and Dowell, E.H., "State Space Modeling for Aeroelastic Panels Subject to Linearized Potential Flow Aerodynamic Loading", AIAA Paper 95-1294, Proceedings of the 36th AIAA/ASME/ASCE/AHS/ASC Structures, Structural Dynamics, and Materials Conference, New Orleans, LA, April 10-13, 1995, Vol. 2, pp. 1183-1189.

8. Kariappa, Somashekar, B.R., and Shah, C.G., "Discrete Element Approach to Flutter of Skew Panels with IN-Plane Forces Under Yawed Supersonic Flow", AIAA Journal, Vol. 8, No. 11, November 1970, pp. 2017-2022.

9. Chowdary, T.V.R., Sinha, P.K., and Parthan, S., "Finite Element Flutter Analysis of Composite Skew Panels", Computers & Structures, Vol. 58, No. 3, pp. 613-620, 1996.

10. Voss, H. M., and Dowell, E. H., "Effect of Aerodynamic Damping on Flutter of Thin Panels", AIAA Journal, Vol. 2, No. 1, January 1964, pp119-120.

11. Lottatti, I., "The Role of Damping on Supersonic Panel Flutter", AIAA Journal, Vol. 23, No. 10, October 1985, pp. 1640-1642.

12. Giles, G.L., "Equivalent Plate Analysis of Aircraft Wing Box Structures with General Planform Geometry", Journal of Aircraft, Vol. 23, No. 11, November 1986, pp. 859-864.

13. Giles, G.L., "Further Generalization of an Equivalent Plate Representation for Aircraft Structural Analysis", Journal of Aircraft, Vol. 26, No. 1, January 1989, pp. 67-74.

14. Livne, E., "Integrated Multidisciplinary Optimization of Actively Controlled Fiber Composite Wings", Ph.D. dissertation, Mechanical, Aerospace and Nuclear Engineering Department, University of California, Los Angeles, 1990.

15. Livne, E., "Analytical Sensitivities for Shape Optimization in Equivalent Plate Structural Wing Models", Journal of Aircraft, Vol. 31, No. 4, pp. 961-969, July-August 1994.

16. Livne, E., and Li, W-L., "Aeroservoelastic Aspects of Wing / Control Surface Planform Shape Optimization", AIAA Journal, Vol. 33, No. 2, February 1995, pp. 302-311.

17. Livne, E., and Milosavljevic, R., "Analytic Sensitivity and Approximation of Skin Buckling Constraints in Wing Shape Synthesis", Journal of Aircraft, Vol. 32, No. 5, September-October 1995, pp. 1102-1113.

18. Li, W-L., and Livne, E., "Analytic Sensitivities and Approximations in Supersonic and Subsonic Wing / Control Surface Unsteady Aerodynamics", AIAA Paper 95-1219, AIAA/ASME/ASCE/AHS/ASC 36th Structures, Structural Dynamics and Materials Conference, New Orleans, April 1995.

19. Haftka, R.T., and Gurdal, Z., "Elements of Structural Optimization", Third Edition, Kluwer Academic Publishers, Dordrecht, Boston, London 1991. (Chapter 6)

20. Pedersen, P., and Seyranian, A., "Sensitivity Analysis for Problems of Dynamic Stability", International Journal of Solids and Structures, Vol. 19, No. 4, pp. 315-335, 1983.

21. Seyranian, A., "Sensitivity Analysis of Multiple Eigenvalues", Mechanical Structures and Machines, Vol. 21, No. 2, pp. 261-284, 1993.

22. Golub, G., and Van Loan, C. F., Matrix Computations, 2nd edition, Johns Hopkins University Press, 1989.

23. Lecina, G., and Petiau, C., "Advances in Optimal Design with Composite Materials", in Computer Aided Optimal Design: Structuyral and Mechanical Systems, C.A. Mota Soares, editor, Springer Verlag, Berlin, 1987, pp. 943-953.

24. Ausman, J.D., Hangen, J.A., and Acevedo, D.A., "Application of a Local Panel Buckling Constraint within Automated Multidisciplinary Structural Analysis and Design", AIAA 92-1116, 1992 Aerospace Design Conference, February 3-6, 1992, Irvine, CA.

25. Bruhn, E.F., Analysis and Design of Flight Vehicle Structures, Tri State Offset Company, 1973, Chapter C5.

26. Whitney, J. M., Structural Analysis of Laminated Anisotropic Plates, Technomic Publishing Company, Lancaster, PA, 1987.

27. Tsai, S.W., and Hahn, H.T., Introduction to Composite Materials, Technomic Publishing Company, Lancaster, PA, 1980.

FLUTTER ANALYSIS AND ANALYTIC SENSITIVITIES
FOR TRAPEZOIDAL PANELS

by

David Mineau

A thesis submitted in partial fulfillment
of the requirements for the degree of

Master of Science
in Aeronautics and Astronautics

University of Washington

1996

Approved by ______________________________
(Chairperson of Supervisory Committee)

Program Authorized
to Offer Degree ______________________________

Date ______________________________

Master's Thesis

In presenting this thesis in partial fulfillment of the requirements for a Master's degree at the University of Washington, I agree that the Library shall make its copies freely available for inspection. I further agree that extensive copying of this thesis is allowable only for scholarly purposes, consistent with "fair use" as prescribed in the U.S. Copyright Law. Any other reproduction for any purposes or by any means shall not be allowed without my written permission.

Signature_______________________________________

Date____

TABLE OF CONTENTS

LIST OF FIGURES

LIST OF TABLES

NOMENCLATURE

$[A]$	in-plane local stiffness matrix for the plate (3 x 3)
$[A_{damp}]$	aerodynamic damping matrix
$[A_{stiff}]$	aerodynamic stiffness matrix
$\left[\overline{\overline{C}}\right]$	total system damping matrix
$[D]$	out of plane local stiffness matrix for the plate (3 x 3)
$f_i(x,y)$	admissible functions
$[F_1],[F_2],[F_3]$	matrices containing admissible functions and their derivatives
$F_B(x,y)$	weight function for admissible functions ensuring zero displacement on panel boundary
F_{ij}^{qp}	coefficients in the polynomial expression for $[F_3]$
$h(x,y)$	total thickness of panel
$\overline{H}(x,y)$	depth of wing
$\overline{H_{ih}}$	coefficients of wing depth polynomial
i,i_1,i_2	indices of terms in layer thickness polynomials
I_{TR}	integral of a simple polynomial term over trapezoidal panel area
$[K],[K_G]$	panel stiffness and geometric stiffness matrix, respectively
$\left[\overline{\overline{K}}\right]$	total system stiffness matrix
m,n	powers of x and y in a polynomial term
m_k^{ti},n_k^{ti}	powers of x and y in polynomial series for thickness of layer i
m_p^w,n_p^w	powers of x and y in Ritz functions
m_h,n_h	powers of x and y in the wing depth series
m_j^v,n_j^v,n_i^u	powers of x and y in polynomial terms of $[F_3]$
$mf2_{ij}^{qp},nf2_{ij}^{qp}$	powers of x and y in elements of $[F_2]$
$\overline{m}_{qw,pw},\overline{n}_{qw,pw}$	powers of x and y for elements of $[\alpha]$
$[M],\left[\overline{\overline{M}}\right]$	panel mass matrix and total system mass matrix

M_∞	free stream Mach number
N_i	number of terms in the thickness polynomial for layer i
N_L	number of layers
$[N]$	2 x 2 matrix of in-plane loads
N_x, N_y, N_{xy}	in-plane loads per unit length
P_ξ, P_t	coefficients associated with piston theory aerodynamics
$[\overline{\overline{Q}}]$	3 x 3 constitutive matrix for a layer
$[Q_i]$	material properties matrix
Q_i	generalized force
$\{Q\}$	vector of generalized forces
$[Q_{stiff}]$, $[Q_{damp}]$	aerodynamic stiffness and damping matrices
$q_p, \{q\}$	generalized displacement and the vector of generalized displacements for panel
q_{flutt}, q_{crit}	flutter dynamic pressures with and without damping, respectively
R, S	coefficients of front line or aft line of panel
$t_i(x,y)$	thickness of layer i
T	kinetic energy of the system
T_j^i	coefficient j in the polynomial series for layer i
U	total potential energy of the system
U_i, V_j	shape dependent coefficients of F_B
U_∞	free stream velocity
$\left[\overline{\overline{U}}\right], \left[\overline{\overline{V}}\right]$	first order state space system matrices
V	potential energy of the panel due to in-plane loads
$W^1(x,y)$	panel elastic out of plane displacement
$W_{qw,pw}$	coefficients of polynomial elements of $[\alpha]$
$[\alpha]$	matrix of function derivatives
δw	virtual work
ϕ	yaw angle of the flow
Λ_{flutt}, Λ_{crit}	normalized flutter dynamic pressures with and without damping
λ	eigenvalue of the aeroelastic system
θ	fiber orientation angle
ρ_∞, ρ_m	free stream density and panel material density
ω	frequency
$\{\psi\},\{\phi\}$	right and left eigenvectors of the generalized eigenvalue problem
ψ	panel skew angle

Ω_{crit} normalized flutter frequency

subscripts

A - aft (rear)

F - front.

L - left

R - right.

ACKNOWLEDGMENTS

Firstly I thank my Lord Jesus, who has blessed me with the ability and opportunity to complete this degree. I would like to express my thanks to Professor Eli Livne for his tremendous vision, guidance, and support during the length of my graduate studies and the preparation of this work. His vast knowledge in all areas of engineering has left a lasting mark on my education and is greatly appreciated. To my wife Amy--thank you so much for your support and love over the last several months. You kept my sanity intact.

CHAPTER 1

INTRODUCTION

A substantial amount of experience and knowledge has been accumulated over the last forty years regarding the aeroelasticity of panels in supersonic flow (Refs. 1-4). Different numerical solution techniques have been used, including exact, as well as approximate Galerkin, Rayleigh-Ritz, and Finite Element techniques (Refs. 5-7). The problem has practical implications associated with the design of high speed aerospace vehicles. As an aeroelastic research problem, it is rich and interesting, encompassing a wealth of phenomena. These include linear and nonlinear stability and dynamic response, dynamics of systems with random parameters (Ref. 8), and interactions between static and dynamic instabilities in the presence of in-plane loads and thermal effects (Refs. 9-10). Panel flutter has been used to study applications of composite materials (Refs. 11-12), transverse shear effects (Refs. 13-14), active aeroelastic control using strain actuators (Refs. 15-16), chaotic dynamics (Refs. 17-18) , and order reduction in unsteady aerodynamics (Ref. 19). Most of the studies in the vast panel flutter literature, however, are confined to rectangular panels. Solution techniques and results for quadrilateral and trapezoidal panels have been discussed in only a small number of articles (Refs. 20-23). Skin panels in typical aerospace structures, however, are very often trapezoidal in shape. Moreover, in the course of optimization of such aerospace structures, internal ribs, spars and stiffeners may be moved to form trapezoidal skin panels, and these panels may change shape during optimization in addition to changing material properties and thicknesses. The capability to efficiently evaluate the aeroelastic stability of trapezoidal skin panels under combined in-plane loads, as well as sensitivities with respect to sizing, material and shape design variables, constitutes an important building block in any overall structural/aeroelastic optimization capability. For optimization strategies based on non-linear programming and approximation concepts (Refs. 24), evaluation of alternative approximation techniques for aeroelastic constraints is required, since very little experience exists in this area.

The optimization of panels, subject to aeroelastic constraints, has been studied in cases involving isotropic and composite construction (Refs. 25-29). These studies are usually limited to the treatment of an isolated panel, excluding its interaction with the structure containing it. In our effort to develop effective aeroservoelastic synthesis techniques for stressed skin aerospace structures, we have ventured into the area of airframe shape optimization in order to make rigorous design optimization available to the designer at an early stage of the design process, where overall shape of the vehicle is still evolving. Analytic shape sensitivities and approximations have been developed for wing box structural modeling, integrated wing box / panel buckling analysis, and unsteady wing aerodynamics in both subsonic and supersonic flight (Refs. 35-38). The present work will focus on the integrated wing box / panel flutter analysis and

sensitivity problem with an emphasis on the needs of planform shape optimization. This includes the sensitivity analysis of panel flutter in the case of the isolated panel, subject to given in-plane loads.

The thesis opens in Chapter 2 with a derivation of the equations of motions for the panel flutter problem based on a Ritz approximation. Chapter 3 discusses the panel modeling and the simple polynomials used as admissible functions in the Ritz analysis. Chapters 4 through 7 develop the mass, stiffness, geometric stiffness, and aerodynamic matrices. Analytic sensitivities with respect to panel shape, thickness, and fiber orientation are derived in Chapter 8. Chapter 9 presents the verification and results of the present technique and Chapter 10 provides the conclusions of the work.

CHAPTER 2

PANEL FLUTTER EQUATIONS OF MOTION

2.1 Introduction

The panel flutter equations and stability analysis are developed in this chapter. The equations of motion are derived using energy methods and Ritz approximation. The formulation uses the assumptions of classical plate theory for symmetric composite laminates. A State Space modeling approach is used to develop the stability analysis of the system, and the flutter problem is shown to be a linear generalized eigenvalue problem. The determination of critical dynamic pressures calculated with and without aerodynamic damping is discussed as well as the different types of aeroelastic instability.

2.2 The Lagrange Equations

The standard Lagrange equations, for a system with N degrees of freedom, is given as:

$$\frac{\partial}{\partial t}\left(\frac{\partial T}{\partial q_{j,t}}\right)-\frac{\partial (T-U)}{\partial q_j}=Q_j \qquad j=1\ldots N \tag{2.1}$$

where q_j are the generalized coordinates, U is the total potential energy of the system, T is the kinetic energy, and Q_j (the generalized forces) are defined by the virtual work of non-conservative forces:

$$\delta w=\sum Q_j \cdot \delta q_j \tag{2.2}$$

In plate theory, the potential energy is usually derived as the sum of the strain energy due to bending, U, and the potential energy due to in-plane loads, V. Thus Equation 2.1 can be written as

$$\frac{\partial (U+V-T)}{\partial q_j}+\frac{\partial}{\partial t}\left(\frac{\partial T}{\partial q_{j,t}}\right)=Q_j \qquad j=1\ldots N \tag{2.3}$$

For a symmetric laminate the strain energy due to bending (Ref. 52) can be written in the form

$$U = \frac{1}{2}\iint \begin{bmatrix} W,^1_{xx} & W,^1_{yy} & 2W,^1_{xy} \end{bmatrix} [D] \begin{bmatrix} W,^1_{xx} \\ W,^1_{yy} \\ 2W,^1_{xy} \end{bmatrix} dxdy \tag{2.4}$$

where $W^1{}_{(x,y,t)}$ is the vertical displacement of the panel and [D] is the symmetric 3X3 bending stiffness matrix defined by

$$D_{ij} = \int_z z^2 Q_{ij} dz \tag{2.5}$$

The potential energy of in-plane loads, N_{ij}, due to the deflection $W^1{}_{(x,y,t)}$ is (Ref. 52)

$$V = \frac{1}{2}\iint \begin{bmatrix} W,^1_x & W,^1_y \end{bmatrix} \begin{bmatrix} N_x & N_{xy} \\ N_{xy} & N_y \end{bmatrix} \begin{bmatrix} W,^1_x \\ W,^1_y \end{bmatrix} dxdy \tag{2.6}$$

Finally, the kinetic energy of the panel is given by

$$T = \frac{1}{2}\iint \rho_m h \left(\frac{\partial W^1}{\partial t} \right)^2 dxdy \tag{2.7}$$

where ρ_m is the material density per unit volume and h(x,y) is the panel thickness.

2.3 Ritz Formulation

The unknown elastic deformation $W^1{}_{(x,y,t)}$ is approximated by a series of admissible functions:

$$W^1(x,y,t) = \sum_{i=1}^{N} f_{i(x,y)} q_i(t) \tag{2.8}$$

The functions $f_{i\,(x,y)}$ satisfy the geometric boundary conditions and $q_{i\,(t)}$ are the generalized displacements. In matrix form the deformation is:

$$W^{1}_{(x,y,t)} = \left\{ f_1\,(\mathrm{x,y}) \quad f_2\,(\mathrm{x,y}) \quad \cdots \quad f_N\,(\mathrm{x,y}) \right\} \begin{Bmatrix} q_1(t) \\ q_2(t) \\ \cdot \\ q_N(t) \end{Bmatrix} = \left[F_1\right]\{q\} \tag{2.9}$$

The first derivatives can be expressed as:

$$\begin{Bmatrix} W^1{}_{,x} \\ W^1{}_{,y} \end{Bmatrix} = \begin{bmatrix} f_{1,x} & f_{2,x} & \cdots & f_{N,x} \\ f_{1,y} & f_{2,y} & \cdots & f_{N,y} \end{bmatrix} \begin{Bmatrix} q_1 \\ q_2 \\ \cdot \\ q_N \end{Bmatrix} = \left[F_2\right]\{q\} \tag{2.10}$$

and the second derivatives are given by:

$$\begin{Bmatrix} W^1{}_{,xx} \\ W^1{}_{,yy} \\ 2W^1{}_{,xy} \end{Bmatrix} = \begin{bmatrix} f_{1,xx} & f_{2,xx} & \cdots & f_{N,xx} \\ f_{1,yy} & f_{2,yy} & \cdots & f_{N,yy} \\ 2f_{1,xy} & 2f_{2,xy} & \cdots & 2f_{N,xy} \end{bmatrix} \begin{Bmatrix} q_1 \\ q_2 \\ \cdot \\ q_N \end{Bmatrix} = \left[F_3\right]\{q\} \tag{2.11}$$

These Ritz approximations, used to reduce the order of the system from infinite to N, can now be substituted into the Lagrange equations.

2.4 Strain Energy

The partial derivative of the strain energy (Eq. 2.4) with respect to the generalized coordinate q_j is:

$$\begin{aligned} \frac{\partial\ U}{\partial\ q_j} = \frac{1}{2}\iint \frac{\partial}{\partial\ q_i}\left(\left[W,^1_{xx} \quad W,^1_{yy} \quad 2W,^1_{xy}\right]\right)\cdot\left[D\right]\begin{bmatrix} W,^1_{xx} \\ W,^1_{yy} \\ 2W,^1_{xy} \end{bmatrix} \\ +\left[W,^1_{xx} \quad W,^1_{yy} \quad 2W,^1_{xy}\right]\left[D\right]\cdot\frac{\partial}{\partial\ q_i}\left(\begin{bmatrix} W,^1_{xx} \\ W,^1_{yy} \\ 2W,^1_{xy} \end{bmatrix}\right)dxdy \end{aligned} \tag{2.12}$$

From equation 2.8 the second derivatives of W^1 can be given as:

$$W,_{xx}^{1} = \sum f_{i,xx} q_i \qquad W,_{yy}^{1} = \sum f_{i,yy} q_i \qquad W,_{xy}^{1} = \sum f_{i,xy} q_i \tag{2.13}$$

from which follows

$$\frac{\partial\, W,_{xx}^{1}}{\partial\, q_j} = f_{j,xx} \qquad \frac{\partial\, W,_{yy}^{1}}{\partial\, q_j} = f_{j,yy} \qquad \frac{\partial\, W,_{xy}^{1}}{\partial\, q_j} = f_{j,xy} \tag{2.14}$$

substituting Eq. 2.14 into Eq. 2.12 gives:

$$\frac{\partial\, U}{\partial\, q_j} = \frac{1}{2}\iint \left[\begin{bmatrix} f_{j,xx} & f_{j,yy} & 2f_{j,xy} \end{bmatrix} [D] \begin{bmatrix} W,_{xx}^{1} \\ W,_{yy}^{1} \\ 2W,_{xy}^{1} \end{bmatrix} + \begin{bmatrix} W,_{xx}^{1} & W,_{yy}^{1} & 2W,_{xy}^{1} \end{bmatrix} [D] \begin{bmatrix} f_{j,xx} \\ f_{j,yy} \\ 2f_{j,xy} \end{bmatrix} \right] dxdy \tag{2.15}$$

Notice that the quantity $\begin{bmatrix} W,_{xx}^{1} & W,_{yy}^{1} & 2W,_{xy}^{1} \end{bmatrix} [D] \begin{bmatrix} f_{j,xx} \\ f_{j,yy} \\ 2f_{j,xy} \end{bmatrix}$ is a 1x1 matrix and is therefore symmetric. Thus

$$\begin{aligned} \begin{bmatrix} W,_{xx}^{1} & W,_{yy}^{1} & 2W,_{xy}^{1} \end{bmatrix} [D] \begin{bmatrix} f_{j,xx} \\ f_{j,yy} \\ 2f_{j,xy} \end{bmatrix} &= \left[\begin{bmatrix} W,_{xx}^{1} & W,_{yy}^{1} & 2W,_{xy}^{1} \end{bmatrix} [D] \begin{bmatrix} f_{j,xx} \\ f_{j,yy} \\ 2f_{j,xy} \end{bmatrix} \right]^T \\ &= \begin{bmatrix} f_{j,xx} & f_{j,yy} & 2f_{j,xy} \end{bmatrix} [D] \begin{bmatrix} W,_{xx}^{1} \\ W,_{yy}^{1} \\ W,_{xy}^{1} \end{bmatrix} \end{aligned} \tag{2.16}$$

Substituting Eq. 2.16 simplifies 2.15 to:

$$\frac{\partial\, U}{\partial\, q_j} = \iint \begin{bmatrix} f_{j,xx} & f_{j,yy} & 2f_{xy} \end{bmatrix} [D] \begin{bmatrix} W,_{xx}^{1} \\ W,_{yy}^{1} \\ 2W,_{xy}^{1} \end{bmatrix} dxdy \tag{2.17}$$

For all j=1...N Eq. 2.17 becomes:

$$\begin{Bmatrix} \dfrac{\partial U}{\partial q_1} \\ \dfrac{\partial U}{\partial q_2} \\ \vdots \\ \dfrac{\partial U}{\partial q_N} \end{Bmatrix} = \iint \begin{bmatrix} f_{1,xx} & f_{1,yy} & 2f_{1,xy} \\ f_{2,xx} & f_{2,yy} & 2f_{2.xy} \\ \vdots & \vdots & \vdots \\ f_{N,xx} & f_{N,yy} & 2f_{N,xy} \end{bmatrix} [D] \begin{bmatrix} W,^1_{xx} \\ W,^1_{yy} \\ 2W,^1_{xy} \end{bmatrix} dxdy \tag{2.18}$$

Substituting Eq. 2.11 gives:

$$\begin{Bmatrix} \dfrac{\partial U}{\partial q_1} \\ \dfrac{\partial U}{\partial q_2} \\ \vdots \\ \dfrac{\partial U}{\partial q_N} \end{Bmatrix} = \iint [F_3]^T [D][F_3]\{q\} dxdy \tag{2.19}$$

2.5 Potential Energy Due to In-plane Forces

The partial derivative of V (Eq. 2.6) with respect to the generalized coordinate q_j is:

$$\frac{\partial V}{\partial q_j} = \frac{1}{2} \iint \frac{\partial}{\partial q_i} \left(\begin{bmatrix} W,^1_x & W,^1_y \end{bmatrix} \right) \cdot [N] \begin{bmatrix} W,^1_x \\ W,^1_y \end{bmatrix} + \begin{bmatrix} W,^1_x & W,^1_y \end{bmatrix} [N] \cdot \frac{\partial}{\partial q_i} \left(\begin{bmatrix} W,^1_x \\ W,^1_y \end{bmatrix} \right) dxdy \tag{2.20}$$

where $[N] = \begin{bmatrix} N_x & N_{xy} \\ N_{xy} & N_y \end{bmatrix}$

From equation 2.8 the first derivatives of W^1 (x,y,t) can be given as:

$$W,^1_x = \sum f_{i,x} q_i \qquad W^1_{,y} = \sum f_{i,y} q_i \tag{2.21}$$

from which follows

$$\frac{\partial\ W,_x^1}{\partial\ q_j} = f_{j,x} \qquad\qquad \frac{\partial\ W,_y^1}{\partial\ q_j} = f_{j,y} \tag{2.22}$$

substituting Eq. 2.22 into 2.20 gives:

$$\frac{\partial\ V}{\partial\ q_j} = \frac{1}{2}\iint \left[f_{j,x} \quad f_{j,y} \right] [N] \begin{bmatrix} W,_x^1 \\ W,_y^1 \end{bmatrix} + \left[W,_x^1 \quad W,_y^1 \right] [N] \begin{bmatrix} f_{j,x} \\ f_{j,y} \end{bmatrix} dxdy \tag{2.23}$$

As in the derivation of the strain energy, the second term in the integral is symmetric because it is a 1x1 matrix. Therefore Eq. 2.23 can be written as:

$$\frac{\partial\ V}{\partial\ q_j} = \iint \left[f_{j,x} \quad f_{j,y} \right] [N] \begin{bmatrix} W,_x^1 \\ W,_y^1 \end{bmatrix} dxdy \tag{2.24}$$

For all j=1...N

$$\begin{Bmatrix} \dfrac{\partial\ V}{\partial\ q_1} \\ \dfrac{\partial\ V}{\partial\ q_2} \\ \vdots \\ \dfrac{\partial\ V}{\partial\ q_N} \end{Bmatrix} = \iint \begin{bmatrix} f_{1,x} & f_{1,y} \\ \vdots & \vdots \\ f_{N,x} & f_{,N,y} \end{bmatrix} [N] \begin{bmatrix} W,_x^1 \\ W,_y^1 \end{bmatrix} dxdy \tag{2.25}$$

Finally substituting Eq. 2.10 into Eq. 2.25 gives:

$$\begin{Bmatrix} \frac{\partial V}{\partial q_1} \\ \frac{\partial V}{\partial q_2} \\ \vdots \\ \frac{\partial V}{\partial q_N} \end{Bmatrix} = \iint [F_2]^T [N][F_2]\{q\} dxdy \tag{2.26}$$

2.6 Kinetic Energy

The kinetic energy in this problem (Eq. 2.7) is a function of the time derivatives of the generalized coordinates only, therefore $\frac{\partial T}{\partial q_j} = 0$.

The derivative of $W^1_{(x,y,t)}$ with respect to time can be written as:

$$\frac{\partial W^1}{\partial t} = \sum_{i=1}^{N} f_i q_{i,t} \tag{2.27}$$

Substituting this expression into Eq. 2.7 results in:

$$T = \frac{1}{2} \iint \rho_m h \left(\sum_{i=1}^{N} f_i q_{i,t} \right)^2 dxdy \tag{2.28}$$

Differentiating with respect to $q_{j,t}$ gives:

$$\frac{\partial T}{\partial q_{j,t}} = \iint \rho_m h f_j \left(\sum_{i=1}^{N} f_i q_{i,t} \right) dxdy \tag{2.29}$$

Differentiating with respect to time gives:

$$\frac{\partial}{\partial t}\left(\frac{\partial T}{\partial q_{j,t}}\right) = \iint \rho_m h f_j \left(\sum_{i=1}^{N} f_i \ddot{q}_i\right) dxdy \tag{2.30}$$

Expanding for j=1...N and substituting in Eq. 2.9 leads to:

$$\left\{\begin{matrix} \frac{\partial}{\partial t}\left(\frac{\partial T}{\partial q_{1,t}}\right) \\ \frac{\partial}{\partial t}\left(\frac{\partial T}{\partial q_{2,t}}\right) \\ \vdots \\ \frac{\partial}{\partial t}\left(\frac{\partial T}{\partial q_{N,t}}\right) \end{matrix}\right\} = \iint \rho_m h \begin{bmatrix} f_1 \\ f_2 \\ \vdots \\ f_N \end{bmatrix} [F_1]\{\ddot{q}\} dxdy = \iint \rho_m h [F_1]^T [F_1]\{\ddot{q}\} dxdy \tag{2.31}$$

where

$$\{\ddot{q}\} = \{q_{,tt}\}$$

2.7 Virtual Work Due to Transverse Loads

The virtual work, δw done by a transverse force, $\bar{q}_{(x,y)}$, on the panel is the force over the panel area multiplied by the virtual distance:

$$\delta w = \iint \delta W^1 \bar{q}_{(x,y)} dxdy \tag{2.32}$$

Using Eq. 2.8 the virtual displacement can be expressed as:

$$\delta W^1 = \sum_{i=1}^{N} f_i \delta q_i$$

Combining the above equations gives:

$$\delta w = \iint \sum_{i=1}^{N} f_i \delta q_i \bar{q}_{(x,y)} dxdy \tag{2.33}$$

By the definition of Q_i (Eq. 2.2), the vector {Q} can be expressed as:

$$\{Q\} = \iint \begin{bmatrix} f_1 \\ \vdots \\ f_N \end{bmatrix} \bar{q}_{(x,y)} dxdy = \iint [F_1]^T \bar{q}_{(x,y)} dxdy \tag{2.34}$$

$\bar{q}_{(x,y)}$ can be any transverse load, but in the context of panel flutter it is the pressure applied to the plate by the aerodynamic flow. Therefore the aerodynamic contribution to the system will be solely through the {Q} vector.

2.8 Equations of Motion

Recall that the Lagrange equation was given by:

$$\frac{\partial (U+V)}{\partial q_j} + \frac{\partial}{\partial t}\left(\frac{\partial T}{\partial q_{j,t}}\right) = Q_i \qquad j = 1 \ldots N$$

Substituting the derived equations above gives:

$$\begin{aligned} &\iint [F_3]^T [D][F_3]\{q\} dxdy + \iint [F_2]^T [N][F_2]\{q\} dxdy + \iint \rho_m h [F_1]^T [F_1]\{\ddot{q}\} dxdy = \\ &\iint [F_1]^T \bar{q}_{(x,y)} dxdy \end{aligned} \tag{2.35}$$

Because the generalized coordinates, {q}, are not functions of x and y they can be placed outside of the integrals. The equations of motion can then be expressed as:

$$[M]\{\ddot{q}\} + [K]\{q\} + [K_G]\{q\} = \{Q\} \tag{2.36}$$

where [M] is the NxN mass matrix:

$$[M] = \iint \rho_m h [F_1]^T [F_1] dxdy \tag{2.37}$$

[K] is the NxN bending stiffness matrix:

$$[K] = \iint [F_3]^T [D][F_3] dxdy \tag{2.38}$$

and $[K_G]$ is the NxN geometric stiffness matrix:

$$[K_G] = \iint [F_2]^T [N][F_2] dxdy \tag{2.39}$$

2.9 Generalized Eigenvalue Problem

It will be shown in Chapter 7 that when piston theory aerodynamics are used for the transverse load contribution, the nonconservative aerodynamic forces are expressed as:

$$\{Q\} = \rho_\infty U_\infty [A_{damp}]\{\dot{q}\} + \rho_\infty U_\infty^2 [A_{stiff}]\{q\} \tag{2.40}$$

Substituting this into Eq. 2.36 gives the equations of motion as:

$$[M]\{\ddot{q}\} - \rho_\infty U_\infty [A_{damp}]\{\dot{q}\} + [K + K_G - \rho_\infty U_\infty^2 A_{stiff}]\{q\} = \{0\} \tag{2.41}$$

or

$$[\overline{M}]\{\ddot{q}\} + [\overline{C}]\{\dot{q}\} + [\overline{K}]\{q\} = \{0\} \tag{2.42}$$

It should be noted that the model presented above does not include any structural damping. This can be added in the form of viscous damping in the $[\overline{\overline{C}}]$ matrix (Ref. 31).

At a given altitude, Mach number, and corresponding speed, and for a given set of in-plane loads obtained from the wing box solution (Ref. 37), the poles of the system can be found to determine if the panel is stable or unstable. Applying the Laplace transform to Eq. 2.42 gives:

$$\left[s^2 \overline{\overline{M}} + s\overline{\overline{C}} + \overline{\overline{K}}\right]\left\{q_{(s)}\right\} = \{0\} \tag{2.43}$$

This is a quadratic eigenvalue problem which can be solved by converting it to a first order problem. Let $\{x_1(s)\} = \{q(s)\}$ and $\{x_2(s)\} = s\{q(s)\}$ then Eq. 2.43 becomes:

$$\begin{aligned} s\{x_1\} &= \{x_2\} \\ \left[\overline{\overline{M}}\right]s\{x_2\} &= -\left[\overline{\overline{K}}\right]\{x_1\} - \left[\overline{\overline{C}}\right]\{x_2\} \end{aligned} \tag{2.44}$$

or

$$\left[\begin{array}{c|c} I & 0 \\ \hline 0 & \left[\overline{\overline{M}}\right] \end{array}\right] s \begin{Bmatrix} x_1 \\ x_2 \end{Bmatrix} = \left[\begin{array}{c|c} 0 & I \\ \hline -\left[\overline{\overline{K}}\right] & -\left[\overline{\overline{C}}\right] \end{array}\right] \begin{Bmatrix} x_1 \\ x_2 \end{Bmatrix} \tag{2.45}$$

If we have N generalized coordinates, {q}, then $\left[\overline{\overline{M}}\right]$, $\left[\overline{\overline{C}}\right]$, and $\left[\overline{\overline{K}}\right]$ are all NxN matrices and the first order equations are a 2Nx2N generalized linear eigenvalue problem of the form:

$$\left[\overline{\overline{U}}\right]\{\phi\} = \lambda \left[\overline{\overline{V}}\right]\{\phi\} \tag{2.46}$$

where λ are the eigenvalues (poles) of the system and $\{\phi\}$ are the corresponding eigenvectors. The eigenvalues and eigenvectors are found using the QZ algorithm (Ref. 42).

2.10 Stability Boundaries

At the given flight conditions and in-plane loads, a panel is stable if all of its poles (eigenvalues) reside in the left side of the Laplace plane. Each pole contributes to a transient motion in the panel of the

form $e^{\lambda t}$. If a pole is written as $\lambda=\sigma+j\omega$, then it contributes a motion of the form $e^{(\sigma+j\omega)t} = e^{\sigma t}(\cos\omega t + j\sin\omega t)$. A pole's contribution to the panel displacement grows with time if its real part, σ, is greater than zero and therefore causes instability in the panel. A complex pole with a positive real part represents an oscillatory instability, or flutter. A purely real pole that is greater than zero is non-oscillatory and corresponds to divergence or buckling. Thus, eigenvalue analysis can capture instability due to either buckling or flutter.

The point at which a panel becomes unstable is usually found by assuming a given Mach number and set of in-plane loads. The dynamic pressure is, then, slowly increased, keeping all other parameters constant. Eigenvalue analysis is repeated for increasing dynamic pressures until a pole crosses into the right hand side of the s-plane (Fig. 2.1). This is equivalent to flying at a constant Mach number while decreasing altitude. The dynamic pressure at which the panel flutters is labeled $q_{flutter}$.

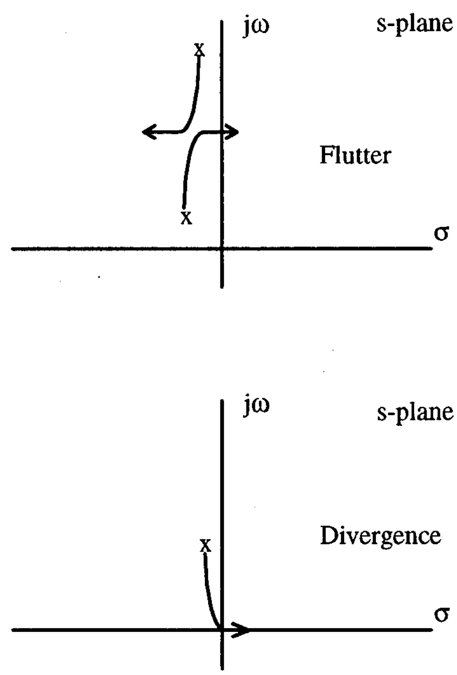

Figure 2.1 Stability Analysis in the Presence of Damping

In the panel flutter literature, it has been observed that due to limitations of Piston Theory, the associated aerodynamic damping can sometimes lead to counter intuitive / unreliable results. Structural damping effects are also quite hard to model accurately(Ref. 31). For a conservative stability boundary, then, the structural and aerodynamic damping are often ignored by setting $\left[\bar{\bar{C}}\right] = [0]$ in Eq. 2.42. This results in a model with no damping, and the stability analysis has to be modified accordingly.

As long as the system is stable its poles are purely imaginary. Only after flutter or buckling occurs does any root have a real part (Fig. 2.2). In the case of flutter, two poles that start out as natural frequencies will coalesce as the dynamic pressure is increased to the point where they become complex conjugates of the form $\pm\sigma + j\omega$ (Fig. 2.2a). The corresponding dynamic pressure is called $q_{critical}$. Buckling or divergence occurs when one root becomes a positive, non-oscillatory root (Fig. 2.2b). The present analysis (and associated computer program) predict both $q_{critical}$ and $q_{flutter}$.

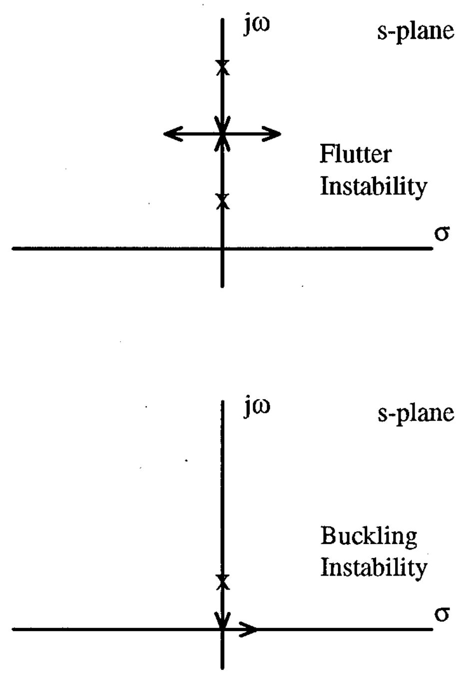

Figure 2.2 Stability Analysis in the Absence of Damping

CHAPTER 3

POLYNOMIAL MODELING

3.1 Introduction

Simple polynomials for modeling and Ritz approximation basis functions are discussed and developed in this chapter. The motivation for using simple polynomials is discussed followed by a presentation of the wing box and panel models used in the present analysis. Finally, admissible polynomials for simply supported panels are developed.

3.2 Motivation for Simple Polynomials

Admissible functions based on simple polynomials, as is well known, lead to ill-conditioned system matrices (Refs. 32-34). As higher order polynomials are introduced to better approximate the solution, high and low order terms appear simultaneously in the system matrices, leading to a large difference in orders of magnitude of matrix terms. On finite word-length computers this leads to ill-conditioned linear equation and eigenvalue solutions. If convergence to the solution is not obtained with low order polynomials, the addition of higher orders will lead to ill-conditioning and the solution technique will likely fail.

However, there are several advantages to simple polynomials if ill-conditioning can be avoided. Simple polynomials allow for integrals in the system matrices to be performed analytically, making numerical quadrature unnecessary. This greatly reduces the computation time required for solution. Simple polynomials have been successfully used as admissible functions in plate vibration and shells. In the context of wing optimization, simple polynomials have been used for deformation, stress, and mode shapes in wings of complex planforms (Ref. 35). Finally, Ref. 37 shows that panel buckling analysis can be successfully integrated with wing box structural analysis using simple polynomials.

The greatest advantage of simple polynomials for the present problem of panel flutter is the ability to perform analytical sensitivities. Refs. 35 and 37 show that it is possible to easily obtain very accurate closed form sensitivities. In design oriented structural analysis there is a need to analyze the flutter stability boundary of the wing panels when their shapes and other design variables are changing. Analytical sensitivities for the stability of wing panels that can be provided quickly to a designer provides an important link in wing and airframe optimization.

The success of previous experiences using simple polynomials for analysis and analytical sensitivities combined with the computational speed such formulation allows is the basis for using simple polynomials in the present panel flutter analysis.

3.3 Modeling

In the polynomial based wing box analysis, the thickness of layers of fibers in different directions is given by simple polynomials. For layer i out of N_L layers in a panel

$$t_i(x,y) = T_1^i + T_2^i x + T_3^i y + T_4^i x^2 + .. = \sum_{k=1}^{N_i} T_k^i \cdot x^{(m_k^t)} \cdot y^{(n_k^t)} \quad , i = 1, N_L \tag{3.1}$$

The powers m_k^t and n_k^t are x and y powers of the k[th] term of the thickness series for the i[th] layer. The coefficients T_k^i serve as sizing type design variables. Unlike many studies, in which wing trapezoidal segments are transformed into a unit square for numerical analysis, here the thickness polynomial is given in terms of the physical x,y coordinates (Fig. 3.1).

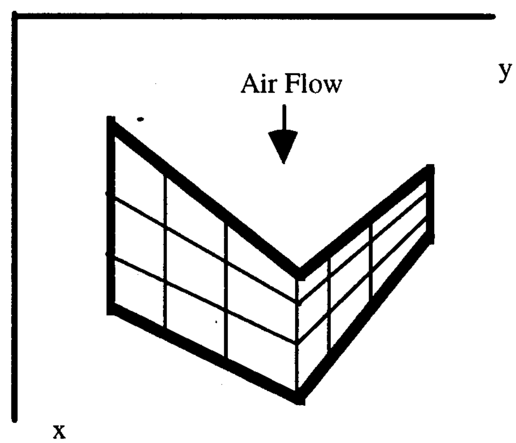

Figure 3.1 Wing Planform

The overall thickness of skin panels is the summation of the N_L layers:

$$h_{(x,y)} = \sum_{i=1}^{N_L} t_i(x,y) = \sum_{i=1}^{N_L} \sum_{k=1}^{N_i} T_k^i \cdot x^{(m_k^{t_i})} \cdot y^{(n_k^{t_i})} \tag{3.2}$$

In a similar manner, cap areas for the spars and ribs of the wing box model are also expressed as simple polynomials of either x (for ribs) or y (for spars) (Refs. 32-34). Depth of the wing box is also given by a simple polynomial in x and y, to be defined later.

3.4 Admissible Functions

An admissible function will be any polynomial we choose that satisfies the simply supported boundary conditions on the perimeter of the panel. Figure 3.2 shows a trapezoidal panel defined by coordinates of its vertices in the x,y axes. The subscripts L and R denote left and right sides, respectively. The subscripts F and A denote front and aft lines, respectively, and x_F and x_A are the x coordinates of the forward and rear points on a line parallel to the sides of the panel.

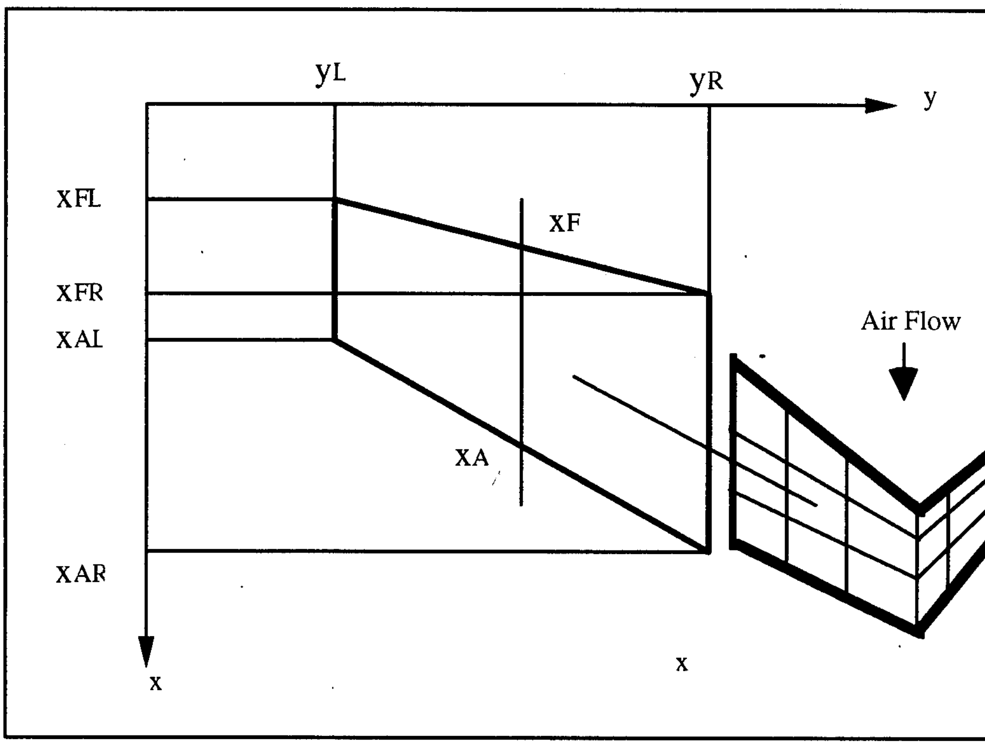

y

Figure 3.2 Panel Layout

Based on Fig. 3.2, we can write the following equation for points on the front line:

$$x_A(y) = \left(\frac{x_{FL}y_R - x_{FR}y_L}{y_R - y_L}\right) + \left(\frac{x_{FR} - x_{FL}}{y_R - y_L}\right)y = R_F + S_F y \tag{3.3}$$

In a similar way, on the rear line, expressing x_A in terms of y leads to:

$$x_A(y) = \left(\frac{x_{AL}y_R - x_{AR}y_L}{y_R - y_L}\right) + \left(\frac{x_{AR} - x_{AL}}{y_R - y_L}\right)y = R_A + S_A y \tag{3.4}$$

The function $F_B(x,y) = \left[x - x_F(y)\right]\left[x - x_A(y)\right]\left[y - y_L\right]\left[y - y_R\right]$ satisfies the zero displacement boundary conditions on the circumference of the panel. Using Eqs. 3.3 and 3.4, and expanding in terms of x and y yields

$$F_{B\,(x,y)} = \left(U_1 + U_2 y + U_3 y^2\right)\{V_1 + V_2 x + V_3 y + V_4 x^2 + V_5 xy + V_6 y^2\} \tag{3.5}$$

or

$$F_{B\,(x,y)} = \sum_{i=1}^{3} U_i y^{n_i^u} \sum_{j=1}^{6} V_j x^{m_j^v} y^{n_j^v} = \sum_{i=1}^{3} \sum_{j=1}^{6} U_i V_j x^{m_j^v} y^{n_i^u + n_j^v} \tag{3.6}$$

where the constants U and V are given in terms of panel vertex coordinates by:

$$\begin{aligned} &U_1 = y_L y_R, U_2 = -(y_L + y_R), U_3 = 1 \\ &V_1 = R_A R_F, V_2 = -\left(R_A + R_F\right), V_3 = \left(R_A S_F + R_F S_A\right) \\ &V_4 = 1, V_5 = -\left(S_A + S_F\right), V_6 = S_F S_A \end{aligned} \tag{3.7}$$

Powers of x and y corresponding to constants U and Vare given in Tables 3.1 and 3.2.

Table 3.1 Constants Ui and their corresponding power of y.

i	U_i	n_i^u
1	U_1	0
2	U_2	1
3	U_3	2

Table 3.2 Constants Vj and their corresponding powers of x and y.

j	V_j	m_j^v	n_j^v
1	V_1	0	0
2	V_2	1	0
3	V_3	0	1
4	V_4	2	0
5	V_5	1	1
6	V_6	0	2

Any polynomial multiplying F_B will be an admissible function satisfying the boundary conditions of a simply supported panel. Therefore the transverse displacement of the panel can be written as:

$$W^1(x,y) = F_B(x,y) \sum_{p=1}^{N_W} q_p x^{m_p^w} y^{n_p^w} \tag{3.8}$$

where the coefficients q_p are the generalized displacements. Substituting the Eq. 3.6 for F_B we can write:

$$W^1(x,y) = \sum_{p=1}^{N_W} q_p \cdot \sum_{i=1}^{3} \sum_{j=1}^{6} U_i V_j x^{(m_j^v + m_p^w)} y^{(n_i^u + n_j^v + n_p^w)} \tag{3.9}$$

The admissible functions are thus expressed in terms of simple polynomials, where the pth admissible function (Eq. 2.8) is given by:

$$f_p(x,y) = \sum_{i=1}^{3} \sum_{j=1}^{6} U_i V_j x^{(m_j^v + m_p^w)} y^{(n_i^u + n_j^v + n_p^w)} \tag{3.10}$$

CHAPTER 4

MASS MATRIX

4.1 Introduction

Equations for the terms of the mass matrix are derived in this chapter. It is shown that the terms can be expressed as linear combinations of area integrals of polynomials.

4.2 Mass Matrix Terms

The mass matrix was derived in Chapter 2 as:

$$[M] = \iint_{area} \rho_m h [F_1]^T [F_1] dxdy \tag{4.1}$$

where ρ_m is the material density per unit volume, $h_{(x,y)}$ is the panel thickness, and the matrix $[F_1]$ contains the admissible functions:

$$[F_1] = [f_1 \quad f_2 \quad \cdots \quad f_N] \tag{4.2}$$

Substituting the admissible functions into [M] gives the individual terms as:

$$M_{rs} = \iint_{area} \rho_m h f_r f_s dxdy \tag{4.3}$$

This equation shows that the mass matrix is symmetric.

The panel thickness, h, is expressed as a summation of the individual layers' thickness. As shown in Chapter 3 the thickness is:

$$h_{(x,y)} = t_{1(x,y)} + t_{2(x,y)} + \ldots + t_{N_L(x,y)} = \sum_{i=1}^{N_L} t_{i(x,y)} = \sum_{i=1}^{N_L} \sum_{k=1}^{N_i} T_k^i x^{m_k^{t_i}} y^{n_k^{t_i}} \tag{4.4}$$

where N_L is the number of layers in the panel and N_i is the number of thickness terms in each layer. If the thickness of all layers are expressed by the same order of complete polynomial then all layers will have the same number of terms, N_t, and the same powers m_k^t and n_k^t. This restriction simplifies the formulation of the panel thickness while not taking away from the flexibility for representing complex panel thickness. A new vector, $\overline{T_k}$ is defined to add all of the T_k^i terms associated with the same powers of x and y:

$$\overline{T_k} = \sum_{i=1}^{N_L} T_k^i \tag{4.5}$$

Now the total panel thickness is simplified as:

$$h_{(x,y)} = \sum_{k=1}^{N_t} \overline{T_k} x^{m_k^t} y^{n_k^t} \tag{4.6}$$

Substituting this into equation (4.3) leads to

$$M_{rs} = \rho_m \sum_{k=1}^{N_t} \overline{T_k} \iint_{area} f_r f_s x^{m_k^t} y^{n_k^t} dxdy \tag{4.7}$$

Recall that the pth admissible function was given in Chapter 3 in terms of the coefficients U_i and V_j as

$$f_{p(x,y)} = \sum_{i=1}^{3} \sum_{j=1}^{6} U_i V_j x^{(m_j^v + m_p^w)} y^{(n_i^u + n_j^v + n_p^w)} \tag{4.8}$$

Substituting into equation (4.7) leads to the explicit form of the mass matrix terms:

$$M_{rs} = \rho_m \sum_{k=1}^{N_t} \sum_{i=1}^{3} \sum_{j=1}^{6} \sum_{ii=1}^{3} \sum_{jj=1}^{6} \overline{T_k} U_i V_j U_{ii} V_{jj} \iint_{area} x^m y^n dxdy \tag{4.9}$$

where

$$m = m_j^v + m_{jj}^v + m_r^w + m_s^w + m_k^t$$

$$n = n_i^u + n_{ii}^u + n_j^v + n_{jj}^v + n_r^w + n_r^w + n_k^t$$

Note that all of the elements of the mass matrix are a linear combination of area integrals of simple polynomials

$$I_{TR(m,n)} = \iint_{area} x^m y^n dxdy \tag{4.10}$$

which, for trapezoidal panels, can be carried out analytically, as shown in detail in Ref . 35. It will be shown that all of the system matrices will be combinations of the same family of integrals $I_{TR(m,n)}$.

The mass matrix is dependent only on the thickness terms T_k^i through $\overline{T_k}$ and the panel shape variables through U_i and V_j. The area integrals depend only on the panel shape variables through the limits of integration as shown in Ref 35.

CHAPTER 5

STIFFNESS MATRIX

5.1 Introduction

Expressions for the terms of the stiffness matrix [K] are derived in this chapter. It is shown that the stiffness terms can be expressed as combinations of integrals of simple polynomials. Quasi homogeneous or orthotropic construction is assumed.

5.2 The In-plane Stiffness Matrix

As shown in Chapter 2, the equation for the Ritz formulation of the stiffness matrix is:

$$[K] = \iint_{area} [F_3]^T [D][F_3] dxdy \tag{5.1}$$

where $[F_3]$ contains the second derivatives of the admissible functions and [D] is the bending stiffness matrix. Expressions for the in-plane stiffness matrix, [A], the bending stiffness matrix and the matrix $[F_3]$ are required for an expression for [K].

The in-plane stiffness matrix is defined as

$$[A] = \int_z [Q(z)] dz \tag{5.2}$$

where [Q(z)] is the material property matrix. [Q(z)] can be expressed in terms of material invarients and the layer fiber orientation angle by defining $[Q_0]$ through $[Q_4]$ (Refs. 37,51) as:

$$\begin{aligned}[Q] = &\begin{bmatrix} U_1 & U_4 & 0 \\ U_4 & U_1 & 0 \\ 0 & 0 & U_5 \end{bmatrix} + U_2 \begin{bmatrix} 1 & 0 & 0 \\ 0 & -1 & 0 \\ 0 & 0 & 0 \end{bmatrix} \cos(2\theta) + U_3 \begin{bmatrix} 1 & -1 & 0 \\ -1 & 1 & 0 \\ 0 & 0 & -1 \end{bmatrix} \cos(4\theta) + \\ &\frac{U_2}{2} \begin{bmatrix} 0 & 0 & 1 \\ 0 & 0 & 1 \\ 1 & 1 & 0 \end{bmatrix} \sin(2\theta) + U_3 \begin{bmatrix} 0 & 0 & 1 \\ 0 & 0 & -1 \\ 1 & -1 & 0 \end{bmatrix} \sin(4\theta)\end{aligned} \tag{5.3}$$

The polynomial description of panel thicknesses in terms of the global x-y coordinates was given in Chapter 3 as a summation of the thickness terms of N_L layers:

$$h_{(x,y)} = t_{1(x,y)} + t_{2(x,y)} + \ldots + t_{N_L(x,y)} = \sum_{i=1}^{N_L} t_{i(x,y)} = \sum_{i=1}^{N_L} \sum_{k=1}^{N_i} T_k^i x^{m_k^{t_i}} y^{n_k^{t_i}} \tag{5.4}$$

For a panel containing N_L layers of fibers, the in-plane stiffness matrix [A] can be expressed in terms of individual layer thicknesses and fiber orientation angles by substituting Eqs. 5.3 and 5.4 into Eq. 5.2:

$$[A]=\sum_{i=1}^{N_L}\Big[[Q_o]+[Q_1]\cos 2\theta_i+[Q_2]\cos 4\theta_i+[Q_3]\sin 2\theta_i+[Q_4]\sin 4\theta_i\Big]\cdot t_{i\,(\mathrm{x,y})} \qquad (5.5)$$

Let a material and fiber orientation dependent matrix, $\left[\overline{\overline{Q}}(\theta_i)\right]$, a 3x3 matrix, be defined as:

$$\left[\overline{\overline{Q}}(\theta_i)\right]=\Big[[Q_o]+[Q_1]\cos 2\theta_i+[Q_2]\cos 4\theta_i+[Q_3]\sin 2\theta_i+[Q_4]\sin 4\theta_i\Big] \qquad (5.6)$$

The in-plane stiffness matrix [A] can now be expressed in terms of the sizing design variables, T^i_j , and fiber directions as a polynomial:

$$[A]=\sum_{i=1}^{N_L}\sum_{k=1}^{N_i}\left[\overline{\overline{Q}}(\theta_i)\right]\cdot x^{(m_k^{t_i})}\cdot y^{(n_k^{t_i})}\cdot T_k^i \qquad (5.7)$$

5.3 The Bending Stiffness Matrix

For unidirectional, orthotropic or quasi homogeneous laminates the in-plane and bending stiffness matrices are related through (Ref. 54)

$$[D]=[A]\frac{h^2}{12} \qquad (5.8)$$

Using Eq 5.4 to express h^2 in terms of thickness design variables, double summation is needed. The indices l_1 and l_2 are used for summation of polynomial terms associated with each layer, as follows:

$$h_{(x,y)}=\sum_{i1=1}^{N_L}\sum_{l1=1}^{N_{i1}}T_{l1}^{i1}\cdot x^{(m_{l1}^{t_{i1}})}\cdot y^{(n_{l1}^{t_{i1}})}=\sum_{i2=1}^{N_L}\sum_{l2=1}^{N_{i2}}T_{l2}^{i2}\cdot x^{(m_{l2}^{t_{i2}})}\cdot y^{(n_{l2}^{t_{i2}})} \qquad (5.9)$$

The bending stiffness matrix, [D], can now be written in polynomial form as

$$[D]=[A]\frac{h^2}{12}=$$

$$\frac{1}{12}\sum_{i=1}^{N_L}\left[\overline{\overline{Q}}(\theta_i)\right]\sum_{i1=1}^{N_L}\sum_{i2=1}^{N_L}\sum_{k=1}^{N_i}\sum_{l1=1}^{N_{i1}}\sum_{l2=1}^{N_{i2}} T_k^i \cdot T_{l1}^{i1} \cdot T_{l2}^{i2} \cdot x^{\left(m_k^{t_i}+m_{l1}^{t_{i1}}+m_{l2}^{t_{i2}}\right)} y^{\left(n_k^{t_i}+n_{l1}^{t_{i1}}+n_{l2}^{t_{i2}}\right)} \tag{5.10}$$

The dependence of [D] on the sizing design variables (thickness coefficients) and fiber angles is now expressed in explicit form.

5.4 The $[F_3]$ Matrix

Recall from Chapter 2 that the $[F_3]$ matrix is defined as:

$$[F_3]=\begin{bmatrix} f_{1,xx} & f_{2,xx} & \cdots & f_{N,xx} \\ f_{1,yy} & f_{2,yy} & \cdots & f_{N,yy} \\ 2f_{1,xy} & 2f_{2,xy} & \cdots & 2f_{N,xy} \end{bmatrix} \tag{5.11}$$

The p[th] admissible function is given as:

$$f_{p(x,y)}=\sum_{i=1}^{3}\sum_{j=1}^{6} U_i V_j x^{(m_j^v+m_p^w)} y^{(n_i^u+n_j^v+n_p^w)} \tag{5.12}$$

Second derivatives of the f_p functions are:

$$f_{p,xx}=\sum_{i=1}^{3}\sum_{j=1}^{6} U_i V_j (m_j^v+m_p^w)(m_j^v+m_p^w-1) x^{(m_j^v+m_p^w-2)} y^{(n_i^u+n_j^v+n_p^w)} \tag{5.13}$$

Note that $f_{p,xx}=0$, if $m_j^v+m_p^w \le 1$. (representing second derivatives of zero order or first order terms) Similarly

$$f_{p,yy}=\sum_{i=1}^{3}\sum_{j=1}^{6} U_i V_j (n_i^u+n_j^v+n_p^w)(n_i^u+n_j^v+n_p^w-1) x^{(m_j^v+m_p^w)} y^{(n_i^u+n_j^v+n_p^w-2)} \tag{5.14}$$

where $f_{p,yy} = 0$, if $n_i^u + n_j^v + n_p^w \leq 1$. Finally

$$2f_{p,xy} = 2\sum_{i=1}^{3}\sum_{j=1}^{6} U_i V_j (m_j^v + m_p^w)(n_i^u + n_j^v + n_p^w) x^{(m_j^v + m_p^w - 1)} y^{(n_i^u + n_j^v + n_p^w - 1)} \tag{5.15}$$

The term $f_{p,xy}$ is set to zero in two cases:

$$2f_{p,xy} = 0, \text{ if } m_j^v + m_p^w = 0, \text{ or } n_i^u + n_j^v + n_p^w = 0$$

The q,p element of $[F_3]$ can be written as:

$$F_{3\,q,p} = \sum_{i=1}^{3}\sum_{j=1}^{6} F_{ij}^{qp} x^{mf_{ij}^{qp}} y^{nf_{ij}^{qp}} \tag{5.16}$$

where the coefficients F_{ij}^{qp} and corresponding powers of x and y, mf_{ij}^{qp} and nf_{ij}^{qp} respectively, are shown in Table 5.1.

Table 5.1 Coefficients and powers of polynomial terms in the $[F_3]$ Matrix

(If any of the power of x and y from columns three and four is less then zero, the corresponding F_{ij}^{qp} element is set to zero)

q (Row of $[F_3]$ Matrix)	F_{ij}^{qp} (Coefficient)	mf_{ij}^{qp} (Power of x)	nf_{ij}^{qp} (Power of y)
1	$U_i V_j (m_j^v + m_p^w) \cdot (m_j^v + m_p^w - 1)$	$m_j^v + m_p^w - 2$	$n_i^u + n_j^v + n_p^w$
2	$U_i V_j (n_i^u + n_j^v + n_p^w) \cdot (n_i^u + n_j^v + n_p^w - 1)$	$m_j^v + m_p^w$	$n_i^u + n_j^v + n_p^w - 2$
3	$U_i V_j \left(m_j^v + m_p^w\right) \cdot \left(n_i^u + n_j^v + n_p^w\right)$	$m_j^v + m_p^w - 1$	$n_i^u + n_j^v + n_p^w - 1$

5.5 The Stiffness Matrix

Equation 5.16 together with Eq. 5.10 are substituted into the equation for the stiffness matrix (Eq. 5.2). The r,s term of the stiffness matrix is:

$$K_{rs} = \sum_{a=1}^{3}\sum_{b=1}^{3} \iint \left(F_{3\,\mathrm{ar}} D_{ab} F_{3\,\mathrm{bs}}\right) dxdy \tag{5.17}$$

and the final expression for the K_{rs} element in polynomial form is:

$$\begin{aligned} K_{rs} = {} & \sum_{a=1}^{3}\sum_{b=1}^{3}\sum_{ii=1}^{3}\sum_{jj=1}^{6}\sum_{iii=1}^{3}\sum_{jjj=1}^{6}\sum_{i=1}^{N_L}\sum_{i1=1}^{N_L}\sum_{i2=1}^{N_L}\sum_{k=1}^{N_i}\sum_{l1=1}^{N_{i1}}\sum_{l2=1}^{N_{i2}} \frac{1}{12} F_{ii,jj}^{a,r} F_{iii,jjj}^{b,s} \cdot \\ & \overline{\overline{Q}}_{a,b}\left(\theta_i\right) T_k^i T_{l1}^{i1} T_{l2}^{i2} \cdot \iint x^{(m_{rs})} y^{(n_{rs})} dxdy \end{aligned} \tag{5.18}$$

where the powers of the x and y terms in the area integral are

$$\begin{aligned} m_{rs} &= mf_{ii,jj}^{a,r} + mf_{iii,jjj}^{b,s} + m_k^{t_i} + m_{l1}^{t_{i1}} + m_{l2}^{t_{i2}} \\ n_{rs} &= nf_{ii,jj}^{a,r} + nf_{iii,jjj}^{b,s} + n_k^{t_i} + n_{l1}^{t_{i1}} + n_{l2}^{t_{i2}} \end{aligned} \tag{5.19}$$

All elements of the stiffness matrix are, thus, linear combinations of the same family of integrals over the panel's area of the form

$$I_{TR}\,(\mathrm{m,n}) = \iint_{Area} x^m y^n dxdy \tag{5.20}$$

Note the explicit dependence on thickness coefficients and fiber directions. The shape dependence is more complex. The coefficients U_i and V_j (Eq. 3.7) depend on the x,y positions of the vertices of the panel. These coefficients, in turn, determine the F coefficients in Table 5.1. In addition, the area integrals (Eq. 5.20) depend on the shape of the panel through the limits of integration.

CHAPTER 6

GEOMETRIC STIFFNESS MATRIX

6.1 Introduction

Equations for the elements of the geometric stiffness matrix are derived in this chapter based on in-plane loads from a wing box structural analysis. It is shown that the geometric stiffness matrix can be expressed as combinations of area integrals of simple polynomials.

6.2 Wing Box Stress Analysis and In-plane Loads

The geometric stiffness matrix was derived in Chapter 2 as:

$$[K_G] = \iint_{area} [F_2]^T [N][F_2] dxdy \tag{6.1}$$

The $[K_G]$ matrix thus depends on the derivatives of the admissible functions contained in $[F_2]$, and the in-plane loads contained in [N]. In classical linear analysis of panels the in-plane loads are assumed given. In the case of wing structures, in-plane loads can be based on wing box stress analysis from standard finite element techniques. In this case, in-plane forces along the sides of the panel are obtained by some functional approximation based on either nodal forces acting on nodes surrounding the panel, or in-plane stresses evaluated for the finite elements surrounding the panel. Alternatively, based on stress distribution in the panel, in-plane loads for buckling analysis can be evaluated throughout the panel, to be integrated over the area of the panel to obtain the matrix $[K_G]$. (Refs. 43-50).

For preliminary design purposes, if the skin panels are small relative to the wing, flutter or buckling analysis may be accurate enough if average N_x, N_y and N_{xy} are used for the panel. These in-plane stresses are assumed constant throughout the panel. This simplifies the integrations in Eq. 6.1, and makes it possible to use interaction formulas for fast approximate buckling analysis (Refs. 45,47 and 49) and 33).

When an equivalent plate modeling approach is used for the wing box analysis (Refs. 32-34), the in-plane skin stresses are obtained from the wing generalized displacements calculated in the wing box stress analysis stage. In the formulation used in Refs. 32-34 admissible Ritz functions for the wing box analysis are given as polynomials in x and y, the global coordinates used to define the planform of the wing and the shape of all panels (Fig. 3.2). In this case, the transverse displacement of the wing is

$$\overline{W}(x,y) = \sum_{i=1}^{\overline{N}_W} x^{\overline{m}_i} y^{\overline{n}_i} \overline{q}_i \tag{6.2}$$

where a bar associates variables with the wing box analysis. The powers $\overline{m_i}$, $\overline{n_i}$, and the number of terms $\overline{N}_w$ are known from the Ritz series used for the wing box displacement solution. The coefficients $\overline{q}_i$, are the generalized wing box displacements. Multiple load cases can be accounted for in the wing analysis, leading to different generalized displacement vectors $\{\overline{q}\}$.

In equivalent plate wing structural analysis based on classical plate theory using Kirchoff's kinematics for a wing with a symmetric cross section, the engineering strains in the x and y directions are given by (Refs 32-34)

$$\begin{aligned}
\overline{\varepsilon_x} &= \frac{\partial \overline{u}}{\partial x} = -z\overline{W}_{,xx} \\
\overline{\varepsilon_y} &= \frac{\partial \overline{v}}{\partial y} = -z\overline{W}_{,yy} \\
\overline{\gamma_{xy}} &= -2z\overline{W}_{,xy}
\end{aligned} \tag{6.3}$$

Let the wing depth be given by $\overline{H}_{(x,y)}$. Then, when skins are thin compared to the depth, they can be assumed located at $z = \pm \overline{H}_{(x,y)}/2$. Focusing on the upper skin, in-plane strains are:

$$\begin{Bmatrix} \overline{\varepsilon}_x \\ \overline{\varepsilon}_y \\ \overline{\gamma}_{xy} \end{Bmatrix} = -\frac{\overline{H}_{(x,y)}}{2} \begin{Bmatrix} \overline{W}_{,xx} \\ \overline{W}_{,yy} \\ 2\overline{W}_{,xy} \end{Bmatrix} \tag{6.4}$$

Now, in a polynomial based formulation for the wing box, the depth of the wing is given in polynomial form

$$\overline{H}(x,y) = \sum_{ih=1}^{N_h} \overline{H}ih \cdot x^{(mh_{ih})} \cdot y^{(nh_{ih})} \tag{6.5}$$

Since the displacement, $\overline{W}_{(x,y)}$ and the depth, $\overline{H}_{(x,y)}$, are polynomial, it is evident (Eq. 6.4), that skin strains due to wing deformation are polynomial too. There are total of N_L layers, each with fiber direction θ_i, and thickness as described by a polynomial equation. The in-plane skin stresses in each layer of the panel are obtained from the strains by the constitutive law:

$$\begin{Bmatrix} \overline{\sigma}_{xx} \\ \overline{\sigma}_{yy} \\ \overline{\sigma}_{xy} \end{Bmatrix}_i = \left[\overline{\overline{Q}}_{(\theta_i)}\right] \begin{Bmatrix} \overline{\varepsilon}_x \\ \overline{\varepsilon}_y \\ \overline{\gamma}_{xy} \end{Bmatrix} \tag{6.6}$$

where $\left[\overline{\overline{Q}}(\theta_i)\right]$ was derived in Chapter 5 as:

$$\left[\overline{\overline{Q}}(\theta_i)\right] = \left[[Q_o] + [Q_1]\cos 2\theta_i + [Q_2]\cos 4\theta_i + [Q_3]\sin 2\theta_i + [Q_4]\sin 4\theta_i\right] \tag{6.7}$$

The in plane loads can now be found in terms of wing box displacements by integration through the thickness of the panel:

$$\begin{Bmatrix} N_x \\ N_y \\ N_{xy} \end{Bmatrix} = \int_z \begin{Bmatrix} \overline{\sigma}_{xx} \\ \overline{\sigma}_{yy} \\ \overline{\sigma}_{xy} \end{Bmatrix} dz = \int_z \left[\overline{\overline{Q}}_{(\theta)}\right] \begin{Bmatrix} \overline{\varepsilon}_x \\ \overline{\varepsilon}_y \\ \overline{\gamma}_{xy} \end{Bmatrix} dz = -\frac{\overline{H}(x,y)}{2} \cdot \int_z \left[\overline{\overline{Q}}_{(\theta)}\right] dz \cdot \begin{Bmatrix} \overline{W}_{,xx} \\ \overline{W}_{,yy} \\ 2\overline{W}_{,xy} \end{Bmatrix} \tag{6.8}$$

The in-plane stiffness matrix is defined as

$$[A] = \int_z [Q(z)] dz \tag{6.9}$$

which was derived in Chapter 4 to be

$$[A] = \sum_{i=1}^{N_L} \sum_{k=1}^{N_i} \left[\overline{\overline{Q}}(\theta_i)\right] \cdot x^{(m_k^{t_i})} \cdot y^{(n_k^{t_i})} \cdot T_k^i \tag{6.10}$$

which leads to

$$\begin{Bmatrix} N_x \\ N_y \\ N_{xy} \end{Bmatrix} = -\frac{\overline{H}}{2}[A] \begin{Bmatrix} \overline{W}_{,xx} \\ \overline{W}_{,yy} \\ 2\overline{W}_{,xy} \end{Bmatrix} \tag{6.11}$$

In order to express Eq. 6.11 in terms of the generalized displacements $\{\overline{q}\}$ calculated in the wing box solution, we define a new vector $\{\alpha\}$ of wing box curvatures:

$$\{\alpha\} = \begin{Bmatrix} \overline{W}_{,xx} \\ \overline{W}_{,yy} \\ 2\overline{W}_{,xy} \end{Bmatrix} = \begin{bmatrix} \cdots & \overline{m}_{pw}\left(\overline{m}_{pw} - 1\right) x^{\overline{m}_{pw}-2} y^{\overline{n}_{pw}} & \cdots \\ \cdots & \overline{n}_{pw}\left(\overline{n}_{pw} - 1\right) x^{\overline{m}_{pw}} y^{\overline{n}_{pw}-2} & \cdots \\ \cdots & \overline{m}_{pw}\,\overline{n}_{pw}\, x^{\overline{m}_{pw}-1} y^{\overline{n}_{pw}-1} & \cdots \end{bmatrix} \begin{Bmatrix} \cdot \\ \cdot \\ \overline{q}_{pw} \\ \cdot \end{Bmatrix} \tag{6.12}$$

where pw is an index for the p'th element in the wing Ritz series. There are $\overline{N}_w$ terms in the Ritz series for wing displacement. The matrix [α] is thus 3 by $\overline{N}_w$. Each element of this matrix is of the form $W_{qw,pw} \cdot x^{(\tilde{m}_{qw,pw})} \cdot y^{(\tilde{n}_{qw,pw})}$, where the coefficient $W_{qw,pw}$, and powers of x and y, $\tilde{m}_{qw,pw}$ and $\tilde{n}_{qw,pw}$ respectively, are described in Table 6.1.

Table 6.1 Coefficients and Powers of x and y of the Matrix [α]

	$W_{qw,pw}$	$\tilde{m}_{qw,pw}$	$\tilde{n}_{qw,pw}$
qw=1 (Row 1 of the Matrix)	$\overline{m}_{pw}(\overline{m}_{pw}-1)$	$\overline{m}_{pw}-2$	$\overline{n}_{pw}$
qw=2 (Row 2 of the Matrix)	$\overline{n}_{pw}(\overline{n}_{pw}-1)$	$\overline{m}_{pw}$	$\overline{n}_{pw}-2$
qw=3 (Row 3 of the Matrix)	$\overline{m}_{pw}\overline{n}_{pw}$	$\overline{m}_{pw}-1$	$\overline{n}_{pw}-1$

When the index qw denotes the row of the matrix (its values varying from 1 to 3) and the index pw specifies terms of the polynomial displacement series for the wing box (varying from 1 to $\overline{N}_w$), then the in-plane load N_x (Eq. 6.11) for the panel can be expressed in polynomial form as

$$N_x = -\frac{\overline{H}}{2}\sum_{qw=1}^{3} A_{1,qw} \cdot \alpha_{qw} = -\frac{\overline{H}}{2}\sum_{qw=1}^{3} A_{1,qw} \sum_{pw=1}^{\overline{N}w} W_{qw,pw}\, x^{\tilde{m}_{qw,pw}}\, y^{\tilde{n}_{qw,pw}}\, \overline{q}_{pw}$$

leading to

$$N_x = -\frac{\overline{H}}{2}\sum_{qw=1}^{3}\sum_{pw=1}^{\overline{N}w} A_{1,qw} W_{qw,pw}\, x^{\tilde{m}_{qw,pw}}\, y^{\tilde{n}_{qw,pw}}\, \overline{q}_{pw} \tag{6.13}$$

Similarly the expressions for N_y and N_{xy} can be derived:

$$N_y = -\frac{\overline{H}}{2}\sum_{qw=1}^{3}\sum_{pw=1}^{\overline{N}w} A_{2,qw} W_{qw,pw}\, x^{\tilde{m}_{qw,pw}}\, y^{\tilde{n}_{qw,pw}}\, \overline{q}_{pw} \tag{6.14}$$

$$N_{xy} = -\frac{\overline{H}}{2}\cdot 2\sum_{qw=1}^{3}\sum_{pw=1}^{\overline{N}w} A_{3,qw} W_{qw,pw}\, x^{\tilde{m}_{qw,pw}}\, y^{\tilde{n}_{qw,pw}}\, \overline{q}_{pw}$$
$$= -\overline{H}\sum_{qw=1}^{3}\sum_{pw=1}^{\overline{N}w} A_{3,qw} W_{qw,pw}\, x^{\tilde{m}_{qw,pw}}\, y^{\tilde{n}_{qw,pw}}\, \overline{q}_{pw} \tag{6.15}$$

Now the polynomial expression for wing depth (Eq. 6.5) can be substituted into Eqs. 6.13-6.15. The general expression for terms of the [N] matrix , $[N]=\begin{bmatrix} N_x & N_{xy} \\ N_{xy} & N_y \end{bmatrix}$, is

$$N_{pp,qq} = -\frac{1}{2}\sum_{ih=1}^{N_h}\sum_{qw=1}^{3}\sum_{pw=1}^{\overline{N}w} A_{ppp,qw} W_{qw,pw} H_{ih}\, x^{(m_{ih}+\tilde{m}_{qw,pw})}\, y^{(n_{ih}+\tilde{n}_{qw,pw})}\, \overline{q}_{pw} \tag{6.16}$$

The indices pp and qq can be either 1 or 2. Note

$$\begin{aligned} &\text{If pp} = 1 \text{ and qq} = 1, \text{ then } A_{ppp,qw} = A_{1,qw} \\ &\text{If pp} = 2 \text{ and qq} = 2, \text{ then } A_{ppp,qw} = A_{2,qw} \\ &\text{When pp} \neq \text{qq}, \; A_{ppp,qw} = 2A_{3,qw} \end{aligned} \tag{6.17}$$

The polynomial expression for the [A] matrix (Eq. 6.10) is now used:

$$N_{pp,qq} = -\frac{1}{2}\sum_{ih=1}^{N_h}\sum_{qw=1}^{3}\sum_{pw=1}^{\overline{N}w}\sum_{i=1}^{N_L}\sum_{k=1}^{N_i} \{\overline{\overline{Q}}_{ppp,qw}(\theta_i)\cdot W_{qw,pw}\cdot$$
$$\cdot H_{ih}\cdot T_k^i\cdot \overline{q}_{pw}\cdot x^{(m_{ih}+mt_k^i+\tilde{m}_{qw,pw})}\cdot y^{(n_{ih}+nt_k^i+\tilde{n}_{qw,pw})}\} \tag{6.18}$$

where the index ppp means the following:

$$\begin{aligned} &\text{If pp} = 1 \text{ and qq} = 1, \text{ then } \overline{\overline{Q}}_{ppp,qw} = \overline{\overline{Q}}_{1,qw} \\ &\text{If pp} = 2 \text{ and qq} = 2, \text{ then } \overline{\overline{Q}}_{ppp,qw} = \overline{\overline{Q}}_{2,qw} \\ &\text{When pp} \neq \text{qq}, \; \overline{\overline{Q}}_{ppp,qw} = 2\overline{\overline{Q}}_{3,qw} \end{aligned} \tag{6.19}$$

The matrix [N], then, can be expressed as a polynomial in x and y according to Eq. 6.18. This equation shows how [N] depends on the wing box solution , the depth of the wing, the thickness coefficients for layers in the panel, material properties and fiber directions. Of course, the wing solution $\{\overline{q}\}$, also depends on depth, thickness of layers, fiber directions and material properties. These affect the

stiffness matrix of the wing as described in Refs. 32-35. It should be emphasized again that polynomial in-plane loads for the flutter analysis can be obtained in a similar manner from wing box analysis based on first order shear deformation plate theory (Refs. 35 and 37) or from finite element results, when skin stresses are approximated by polynomials using least square fitting (Ref. 39)

6.3 The $[F_2]$ Matrix

The $[F_2]$ matrix was defined in Chapter 2 as

$$[F_2] = \begin{bmatrix} f_{1,x} & f_{2,x} & \cdots & f_{N,x} \\ f_{1,y} & f_{2,y} & \cdots & f_{N,y} \end{bmatrix} \tag{6.20}$$

The pth admissible function is defined in Chapter 3 as:

$$f_{p(x,y)} = \sum_{i=1}^{3}\sum_{j=1}^{6} U_i V_j x^{(m_j^v + m_p^w)} y^{(n_i^u + n_j^v + n_p^w)} \tag{6.21}$$

The first derivatives are simply

$$f_{p,x} = \sum_{i=1}^{3}\sum_{j=1}^{6} U_i V_j \left(m_p^w + m_j^v\right) x^{(m_p^w + m_j^v - 1)} \cdot y^{(n_p^w + n_i^u + n_j^v)} \tag{6.22}$$

$$f_{p,y} = \sum_{i=1}^{3}\sum_{j=1}^{6} U_i V_j \left(n_p^w + n_i^u + n_j^v\right) x^{(m_p^w + m_j^v)} \cdot y^{(n_p^w + n_i^u + n_j^v - 1)} \tag{6.23}$$

Thus, the element q,p of the matrix $[F_2]$ is of the form:

$$F_{2\,(q,p)} = \sum_{i=1}^{3}\sum_{j=1}^{6} \tilde{F}2_{i,j}^{q,p} \cdot x^{(mf2_{i,j}^{q,p})} \cdot y^{(nf2_{i,j}^{q,p})} \tag{6.24}$$

The coefficients $\tilde{F}2_{i,j}^{q,p}$ and powers of x and y, $mf2_{i,j}^{q,p}$ and $nf2_{i,j}^{q,p}$, defining the elements of the $[F_2]$ matrix, are described in the table 6.2.

Table 6.2 Coefficients and Powers of Terms of the [F2] Matrix

	$\tilde{F}_{2i,j}^{q,p}$	$mf2_{i,j}^{q,p}$	$nf2_{i,j}^{q,p}$
q=1 (Row 1 of [F2] Matrix)	$U_i V_j (m_p^w + m_j^v)$	$m_p^w + m_j^v - 1$	$n_p^w + n_i^u + n_j^v$
q=2 (Row 2 of [F2] Matrix)	$U_i V_j (n_p^w + n_i^u + n_j^v)$	$m_p^w + m_j^v$	$n_p^w + n_i^u + n_j^v - 1$

6.4 The Geometric Stiffness Matrix

Elements of the matrix $[K_G]$ can now be expressed in polynomial form as follows:

$$K_{G\,r,s} = \iint \sum_{a=1}^{2} \sum_{b=1}^{2} F_{2\,a,r} N_{a,b} F_{2\,b,s} dxdy \tag{6.25}$$

The indices r and s identify terms in the panel Ritz displacement series for the panel. Using polynomial expressions for $[F_2]$ and [N] (Eqs. 6.18 and 6.22), the r,s element of $[K_G]$ is written as:

$$K_{G\,r,s} = -\frac{1}{2} \sum_{a=1}^{2} \sum_{b=1}^{2} \sum_{i=1}^{3} \sum_{j=1}^{6} \sum_{ii=1}^{3} \sum_{jj=1}^{6} \sum_{ih=1}^{N_h} \sum_{qw=1}^{3} \sum_{pw=1}^{\overline{N}w} \sum_{it=1}^{N_L} \sum_{k=1}^{Nt_i} \tilde{F}_{2i,j}^{a,r} \cdot \tilde{F}_{2ii,jj}^{b,s} \cdot$$
$$\cdot \overline{\overline{Q}}_{ppp,qw} (\theta_{it}) \cdot W_{qw,pw} \cdot H_{ih} \cdot T_k^{it} \cdot \bar{q}_{pw} \cdot \iint x^{(mG_{r,s})} y^{(nG_{r,s})} dxdy \tag{6.26}$$

where

$$mG_{r,s} = mf2_{i,j}^{a,r} + mf2_{ii,jj}^{b,s} + m_{ih} + mt_k^{it} + \tilde{m}_{qw,pw}$$
$$nG_{r,s} = nf2_{i,j}^{a,r} + nf2_{ii,jj}^{b,s} + n_{ih} + nt_k^{it} + \tilde{n}_{qw,pw}$$

The index ppp used in $\overline{\overline{Q}}_{pppqw}(\theta_k)$ is defined in Eq. 6.19. As in the case of the mass and stiffness matrices, the geometric stiffness matrix is represented as summation of surface integrals of polynomial terms calculated over the area of the panel. Integrals of the same family

$$I_{TR}(m,n) = \iint_{Area} x^m y^n dxdy \tag{6.27}$$

are used. Evaluation of these integrals is accomplished using the same subroutines used in the wing analysis and all panel matrix analysis.

6.5 Further Discussion of Integration With Wing Structural Analysis

Recall that the results of the wing analysis affect analysis of the panel through the in-plane load matrix [N]. This matrix is obtained by integrating skin stresses (due to wing deformation) through the thickness of the skin, and the resulting N_x, N_y and N_{xy} are functions of x and y as evident in Eqs. 6.18 and 6.19. Now, while equivalent plate wing structural analysis leads to good skin stress predictions in stiff, low aspect ratio wings (Refs. 32-34), still equilibrium is not guaranteed for isolated skin panels. Thus, the in-plane loads (as given by Eq. 6.18) are generally not in equilibrium (This problem is not encountered when wing analysis is based on the finite element method, when in-plane loading on the circumference of an isolated panel is determined from nodal forces on that circumference).

One way to avoid this difficulty and simplify the geometric stiffness matrix is to use an average in-plane loading to be assumed constant over the panel (Ref. 49). If point (x_0, y_0) inside the panel is used to evaluate these average in-plane loads, then the elements of [N] become

$$N_{pp,qq} = -\frac{1}{2}\sum_{ih=1}^{N_h}\sum_{qw=1}^{3}\sum_{pw=1}^{\overline{N}w} A_{ppp,qw} W_{qw,pw} H_{ih} x_0^{(m_{ih}+\tilde{m}_{qw,pw})} y_0^{(n_{ih}+\tilde{n}_{qw,pw})} \overline{q}_{pw} \tag{6.28}$$

The expression for elements of the geometric stiffness matrix (Eq. 6.24) has to be modified, since terms including x_0 and y_0 become constant for the area integration, and can be taken out of the integral.

$$\begin{aligned} K_{G\,r,s} = -\frac{1}{2}\sum_{a=1}^{2}\sum_{b=1}^{2}\sum_{i=1}^{3}\sum_{j=1}^{6}\sum_{ii=1}^{3}\sum_{jj=1}^{6}\sum_{ih=1}^{N_h}\sum_{qw=1}^{3}\sum_{pw=1}^{\overline{N}w}\sum_{it=1}^{N_L}\sum_{k=1}^{Nt_i} & \tilde{F}_{2i,j}^{a,r} \cdot \tilde{F}_{2ii,jj}^{b,s} \cdot \\ & \overline{\overline{Q}}_{ppp,qw}\,(\theta_{it}) \cdot W_{qw,pw} \cdot H_{ih} \cdot T_k^{it} \overline{q}_{pw} \cdot \\ & x_0^{(m_{ih}+\tilde{m}_{qw,pw})} \cdot y_0^{(n_{ih}+\tilde{n}_{qw,pw})} \cdot \\ & \iint x^{(mf2_{i,j}^{a,r}+mf2_{ii,jj}^{b,s}+mt_k^{it})} \cdot y^{(nf2_{i,j}^{a,r}+nf2_{ii,jj}^{b,s}+nt_k^{it})}\, dxdy \end{aligned} \tag{6.29}$$

CHAPTER 7

AERODYNAMIC FORCE MATRICES

7.1 Introduction

The explicit expressions for the terms of the aerodynamic force matrices are derived in this chapter. It is shown that the aerodynamic damping and stiffness matrices can be formulated as combinations of area integrals of simple polynomials. First order linear piston theory aerodynamics is used for the formulation of the matrices. At the conclusion of the chapter the characteristics of the aerodynamic matrices are discussed.

7.2 Piston Theory

As shown in Chapter 2, the aerodynamic contribution to the panel aeroelastic system is given by

$$\{Q\}=\iint_{area}[F_1]^T q(x.y)dxdy \tag{7.1}$$

where q(x,y) is the change in pressure, Δp. First order linear piston theory (Ref. 1) approximates Δp by

$$\Delta p = \frac{\rho_\infty U_\infty^2}{\sqrt{M_\infty^2 - 1}}\left\{W_{,\xi}^1 + \frac{M_\infty^2 - 2}{M_\infty^2 - 1}\frac{1}{U_\infty}W_{,t}^1\right\} \tag{7.2}$$

where ρ_∞, U_∞, and M_∞ are the free stream density, velocity, and Mach number, and ξ is the flow direction.

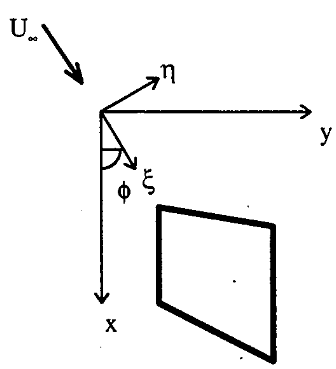

Figure 7.1 Panel in Angled Flow

The simple relation between directional derivatives in the (ξ,η) and (x,y) planes is

$$\frac{\partial}{\partial \xi} = \cos\phi \frac{\partial}{\partial x} + \sin\phi \frac{\partial}{\partial y} \tag{7.3}$$

Simplifying Eq. 7.2, piston theory can be rewritten as:

$$\Delta p = P_\xi \cos\phi W^1_{,x} + P_\xi \sin\phi W^1_{,y} + P_t W^1_{,t} \tag{7.4}$$

where

$$P_\xi = \frac{\rho_\infty U_\infty^2}{\sqrt{M_\infty^2 - 1}} \tag{7.5}$$

$$P_t = P_\xi \frac{M_\infty^2 - 2}{M_\infty^2 - 1} \frac{1}{U_\infty} \tag{7.6}$$

7.3 Aerodynamic Force Matrices

To express the aerodynamic forces in terms of the generalized coordinates the panel displacement terms and their derivatives are expressed as:

$$W^1(x,y) = \left\{ f_{1(x,y)} \quad f_{2(x,y)} \quad \cdots \quad f_{N(x,y)} \right\} \begin{Bmatrix} q_1 \\ q_2 \\ \cdot \\ q_N \end{Bmatrix} = [F_1]\{q\}$$

$$W^1_{,x}(x,y) = \left\{ f_{1,x} \quad f_{2,x} \quad \cdots \quad f_{N,x} \right\} \begin{Bmatrix} q_1 \\ q_2 \\ \cdot \\ q_N \end{Bmatrix} = [F_{1,x}]\{q\}$$

$$W^1_{,y}(x,y) = \left\{ f_{1,y} \quad f_{2,y} \quad \cdots \quad f_{N,y} \right\} \begin{Bmatrix} q_1 \\ q_2 \\ \cdot \\ q_N \end{Bmatrix} = [F_{1,y}]\{q\} \tag{7.7}$$

$$W_{,t}(x,y) = \begin{Bmatrix} f_1 & f_2 & \cdots & f_N \end{Bmatrix} \begin{Bmatrix} q_{1,t} \\ q_{2,t} \\ \cdot \\ q_{N,t} \end{Bmatrix} = [F_1]\{q_{,t}\}$$

Substituting Eqs. 7.4 and 7.7 into Eq. 7.1 gives:

$$\{Q\} = P_\xi \cos\phi \iint_{area} [F_1]^T [F_{1,x}]\{q\}\ dxdy + P_\xi \sin\phi \iint_{area} [F_1]^T [F_{1,y}]\{q\}\ dxdy +$$

$$P_t \iint_{area} [F_1]^T [F_1]\{q_{,t}\}\ dxdy \tag{7.8}$$

It is natural at this point to break up the aerodynamic force into an aerodynamic stiffness matrix and an aerodynamic damping matrix.

$$\{Q\} = P_\xi [Q_{stiff}]\{q\} + P_t [Q_{damp}]\{q_{,t}\} \tag{7.9}$$

where

$$Q_{stiff\ rs} = \cos\phi \iint_{area} f_r f_{s,x}\ \ dxdy + \sin\phi \iint_{area} f_r f_{s,y}\ \ dxdy \tag{7.10}$$

$$Q_{damp\ rs} = \iint_{area} f_r f_s dxdy \tag{7.11}$$

f_r and f_s are the r^{th} and s^{th} admissible functions. In chapter 3 the admissible functions were derived in terms of the coefficients U_i and V_j as

$$f_{p(x,y)} = \sum_{i=1}^{3} \sum_{j=1}^{6} U_i V_j x^{(m_j^v + m_p^w)} y^{(n_i^u + n_j^v + n_p^w)} \tag{7.12}$$

The first derivatives of the admissible functions with respect to x and y are

$$f_{p,x} = \sum_{i=1}^{3} \sum_{j=1}^{6} U_i V_j (m_j^v + m_p^w) x^{(m_j^v + m_p^w - 1)} y^{(n_i^u + n_j^v + n_p^w)} \tag{7.13}$$

$$f_{p,y} = \sum_{i=1}^{3}\sum_{j=1}^{6} U_i V_j (n_i^u + n_j^v + n_p^w) x^{(m_j^v + m_p^w)} y^{(n_i^u + n_j^v + n_p^w - 1)} \tag{7.14}$$

Substituting these into Eqs. 7.10 and 7.11 shows the final expression for the elements of the aerodynamic damping and stiffness matrices.

$$\begin{aligned} Q_{stiff\ \ rs} = {} & \cos\phi \sum_{i=1}^{3}\sum_{j=1}^{6}\sum_{ii=1}^{3}\sum_{jj=1}^{6} U_i V_j U_{ii} V_{jj} (m_{jj}^v + m_s^w) \iint_{area} x^{m-1} y^n dxdy + \\ & \sin\phi \sum_{i=1}^{3}\sum_{j=1}^{6}\sum_{ii=1}^{3}\sum_{jj=1}^{6} U_i V_j U_{ii} V_{jj} (n_{ii}^u + n_{jj}^v + n_s^w) \iint_{area} x^m y^{n-1} dxdy \end{aligned} \tag{7.15}$$

$$Q_{damp\ \ rs} = \sum_{i=1}^{3}\sum_{j=1}^{6}\sum_{ii=1}^{3}\sum_{jj=1}^{6} U_i V_j U_{ii} V_{jj} \iint_{area} x^m y^n dxdy \tag{7.16}$$

where

$$m = (m_j^v + m_{jj}^v + m_r^w + m_s^w)$$

$$n = (n_i^u + n_{ii}^u + n_j^v + n_{jj}^v + n_r^w + n_s^w)$$

The elements of the aerodynamic stiffness and damping matrices are linear combinations of the same integrals as the mass, stiffness, and geometric stiffness matrices.

The aerodynamic stiffness matrix is dependent on the air stream angle, ϕ, the dynamic pressure and Mach number through P_ξ, and the panel shape variables through U_i and V_j. The aerodynamic stiffness matrix is dependent on the dynamic pressure and Mach number through P_t, and the panel shape variables through U_i and V_j. Of course the area integrals themselves depend on the panel's planform shape variables.

In the stability analysis, as shown in Chapter 2, it is convenient for the eigenvalue problem to express the aerodynamic matrices in the form:

$$\begin{aligned} \left[A_{stiff}\right] &= \frac{1}{\sqrt{M_\infty^2 - 1}}\left[Q_{stiff}\right] \\ \left[A_{dampf}\right] &= \frac{1}{\sqrt{M_\infty^2 - 1}} \frac{M_\infty^2 - 2}{M_\infty^2 - 1}\left[Q_{dampf}\right] \end{aligned} \tag{7.17}$$

which leads to an expression for the aerodynamic generalized forces in the form:

$$\{Q\} = \rho_\infty U_\infty \left[A_{damp}\right]\{q_{,t}\} + \rho_\infty U_\infty^2 \left[A_{stiff}\right]\{q\} \tag{7.18}$$

<u>7.4 Characteristics of the Aerodynamic Matrices</u>

Both Q_{stiff} and Q_{damp} have interesting characteristics. Looking at Eq. 7.11 it is obvious that Q_{damp} is a symmetric matrix - a fact which allows faster computation. As a matter of fact, if the panel is made of a single material, and has a constant thickness, the aerodynamic damping matrix is proportional to the mass matrix.

As to the matrix Q_{stiff} - with the current choice of admissible functions (for the simply supported case) this matrix is a skewed symmetric. In addition, certain elements in this matrix are identically zero.

The skew-symmetry of Q_{stiff} is shown by applying integration by parts with respect to x and y to Eq. 7.10:

$$Q_{stiff\ \ rs} = \cos\phi \int_y \left[f_r f_s \Big|_{x1}^{x2} - \int_x f_s f_{r,x} dx \right] dy + \sin\phi \int_x \left[f_r f_s \Big|_{y1}^{y2} - \int_y f_s f_{r,y} dy \right] dx \tag{7.19}$$

Because the admissible functions are zero along the boundaries, the boundary terms are zero leaving

$$Q_{stiff\ \ rs} = -\cos\phi \iint_{area} f_s f_{r,x} \quad dxdy - \sin\phi \iint_{area} f_s f_{r,y} \quad dxdy$$

Clearly:

$$Q_{stiff\ \ rs} = -Q_{stiff\ \ sr} \tag{7.20}$$

It can also be shown that several terms including all the diagonal terms in the aerodynamic stiffness matrix are zero. Starting from Eq. 7.10 with r=s:

$$Q_{stiff\ \ rr} = \cos\phi \iint_{area} f_r f_{r,x} \quad dxdy + \sin\phi \iint_{area} f_r f_{r,y} \quad dxdy \tag{7.21}$$

Looking at the integrands:

$$\int_x f_r f_{r,x}\, dx = \int_x \frac{1}{2}\frac{\partial}{\partial x}\left(f_r^2\right) dx = \frac{1}{2} f_r^2 \Big|_{x_1}^{x_2} = 0$$

and

$$\int_y f_r f_{r,y}\, dy = \int_y \frac{1}{2}\frac{\partial}{\partial y}\left(f_r^2\right)dy = \frac{1}{2} f_r^2\Big|_{y_1}^{y_2} = 0 \tag{7.22}$$

Therefore any diagonal term is identically zero. Of course, the diagonal elements of any skew-symmetric matrix are zero. However, the derivation above serves to illustrate how other terms in the present formulation may be identically zero. For example, if the flow is directed along the x axis, $\sin\phi=0$, two admissible functions may be

$$f_r = f_B(x,y)\cdot x^m$$

and

$$f_s = f_B(x,y)\cdot x^m y^n$$

Thus, in effect for this special case

$$f_s = f_r \cdot y^n$$

Now, the area integral associated with the r,s element of the aerodynamic stiffness matrix is

$$\iint f_r \cdot f_{s,x} dxdy = \iint f_r \cdot f_r \cdot y^n dxdy = \iint \frac{1}{2}\cdot\frac{\partial\,(f_r^2)}{\partial\, x} y^n dxdy$$

Integration in the x direction will immediately show that in the case of simply supported panels ($f_B(x,y)=0$ on the boundary) this area integral is zero. Thus, using complete polynomials as the functions to multiply $f_B(x,y)$ some f_r and f_s have the same powers of x or y for $r \neq s$. For these terms, and depending on the flow direction, the x or y derivative components of $Q_{stiff\ rs}$ will also be zero.

CHAPTER 8

ANALYTIC SENSITIVITIES

8.1 Introduction

Expressions for the analytical sensitivities of the system matrices with respect to the design variables are derived in this chapter. Eigenvalue sensitivities and flutter speed sensitivities are also developed.

8.2 Mass Matrix Sensitivities

The mass matrix is dependent on the panel thickness design variables and the shape design variables. The explicit expression for the mass matrix (Eq. 4.9) allows for easy determination of these analytical sensitivities.

8.2.1 Mass Sensitivities With Respect to Thickness Design Variables T_k^i

The mass matrix is dependent on T_k^i, the sizing variable corresponding to the k^{th} term of the i^{th} layer, through the vector $\overline{T_k}$ (Eq. 4.9). The derivative of a mass matrix term is given as:

$$\frac{\partial M_{rs}}{\partial T_k^i} = \frac{\partial M_{rs}}{\partial \overline{T}_k}\frac{\partial \overline{T}_k}{\partial T_k^i} \tag{8.1}$$

Recall $\overline{T_k}$ is defined as:

$$\overline{T_k} = \sum_{i=1}^{N_L} T_k^i \tag{8.2}$$

Therefore, for a given layer, i, and thickness term, k,

$$\frac{\partial \overline{T}_k}{\partial T_k^i} = 1 \tag{8.3}$$

Substituting this back into Eq. 8.1 shows that

$$\frac{\partial M_{rs}}{\partial T_k^i} = \frac{\partial M_{rs}}{\partial \overline{T}_k} \tag{8.4}$$

for every layer i. Differentiating Eq. 4.9 for any specific k and i gives:

$$\frac{\partial M_{rs}}{\partial T_k^i} = \frac{\partial M_{rs}}{\partial \overline{T}_k} = \rho_m \sum_{i=1}^{3}\sum_{j=1}^{6}\sum_{ii=1}^{3}\sum_{jj=1}^{6} U_i V_j U_{ii} V_{jj} \iint_{area} x^m y^n dxdy \tag{8.5}$$

where

$$m = m_j^v + m_{jj}^v + m_r^w + m_s^w + m_k^t$$

$$n = n_i^u + n_{ii}^u + n_j^v + n_{jj}^v + n_r^w + n_r^w + n_k^t$$

Notice that if all $\frac{\partial M_{rs}}{\partial \overline{T}_k}$ are calculated before the mass matrix, then the mass matrix can be formed as:

$$M_{rs} = \sum_{k=1}^{N_t} \overline{T}_k \frac{\partial M_{rs}}{\partial \overline{T}_k} \tag{8.6}$$

This allows for the mass matrix and its thickness sensitivities to be calculated at the same time with no additional computations that would be required by calculating the mass matrix alone.

8.2.2 Mass Sensitivities With Respect to Shape Design Variables y_L, y_R, x_{FL}, x_{FR}, x_{AL}, and x_{AR}

The mass matrix is dependent on the shape variables through the coefficients U_i and V_j (Eq. 3.7) and the integrals $I_{TR(m,n)}$ because the limits of integration depend on the shape variables (Eq. 4.10). Analytical sensitivities for U_i and V_j are obtained through direct differentiation of Eq. 3.7:

Derivatives with respect to y_L

$$\frac{\partial U_1}{\partial y_L} = y_R$$

$$\frac{\partial U_2}{\partial y_L} = -1$$

$$\frac{\partial U_3}{\partial y_L} = 0$$

$$\frac{\partial V_1}{\partial y_L} = \frac{x_{AL} y_R - x_{AR} y_R}{(y_R - y_L)^2} R_F + \frac{x_{FL} y_R - x_{FR} y_R}{(y_R - y_L)^2} R_A \tag{8.7}$$

$$\frac{\partial V_2}{\partial y_L} = -\frac{x_{AL} y_R - x_{AR} y_R}{(y_R - y_L)^2} - \frac{x_{FL} y_R - x_{FR} y_R}{(y_R - y_L)^2}$$

$$\frac{\partial V_3}{\partial y_L} = \frac{x_{FL} y_R - x_{FR} y_R}{(y_R - y_L)^2} S_A + \frac{x_{AR} - x_{AL}}{(y_R - y_L)^2} R_F + \frac{x_{AL} y_R - x_{AR} y_R}{(y_R - y_L)^2} S_F + \frac{x_{FR} - x_{FL}}{(y_R - y_L)^2} R_A$$

$$\frac{\partial V_4}{\partial y_L} = 0$$

$$\frac{\partial V_5}{\partial y_L} = -\frac{x_{FR} - x_{FL}}{(y_R - y_L)^2} - \frac{x_{AR} - x_{AL}}{(y_R - y_L)^2}$$

$$\frac{\partial V_6}{\partial y_L} = \frac{x_{FR} - x_{FL}}{(y_R - y_L)^2} S_A + \frac{x_{AR} - x_{AL}}{(y_R - y_L)^2} S_F$$

Derivatives with respect to y_R

$$\frac{\partial U_1}{\partial y_R} = y_L$$

$$\frac{\partial U_2}{\partial y_R} = -1$$

$$\frac{\partial U_3}{\partial y_R} = 0$$

$$\frac{\partial V_1}{\partial y_R} = \frac{x_{AR} y_L - x_{AL} y_L}{(y_R - y_L)^2} R_F + \frac{x_{FR} y_L - x_{FL} y_L}{(y_R - y_L)^2} R_A$$

$$\frac{\partial V_2}{\partial y_R} = -\frac{x_{AR} y_L - x_{AL} y_L}{(y_R - y_L)^2} - \frac{x_{FR} y_L - x_{FL} y_L}{(y_R - y_L)^2} \tag{8.8}$$

$$\frac{\partial V_3}{\partial y_R} = \frac{x_{FR} y_L - x_{FL} y_L}{(y_R - y_L)^2} S_A + \frac{x_{AL} - x_{AR}}{(y_R - y_L)^2} R_F + \frac{x_{AR} y_L - x_{AL} y_L}{(y_R - y_L)^2} S_F + \frac{x_{FL} - x_{FR}}{(y_R - y_L)^2} R_A$$

$$\frac{\partial V_4}{\partial y_R} = 0$$

$$\frac{\partial V_5}{\partial y_R} = -\frac{x_{FL} - x_{FR}}{(y_R - y_L)^2} - \frac{x_{AL} - x_{AR}}{(y_R - y_L)^2}$$

$$\frac{\partial V_6}{\partial y_R} = \frac{x_{FL} - x_{FR}}{(y_R - y_L)^2} S_A + \frac{x_{AL} - x_{AR}}{(y_R - y_L)^2} S_F$$

Derivatives with respect to x_{AL}

$$\frac{\partial U_1}{\partial x_{AL}} = 0$$

$$\frac{\partial U_2}{\partial x_{AL}} = 0$$

$$\frac{\partial U_3}{\partial x_{AL}} = 0$$

$$\frac{\partial V_1}{\partial x_{AL}} = \frac{y_R}{y_R - y_L} R_F$$

$$\frac{\partial V_2}{\partial x_{AL}} = -\frac{y_R}{y_R - y_L} \tag{8.9}$$

$$\frac{\partial V_3}{\partial x_{AL}} = \frac{-1}{y_R - y_L} R_F + \frac{y_R}{y_R - y_L} S_F$$

$$\frac{\partial V_4}{\partial x_{AL}} = 0$$

$$\frac{\partial V_5}{\partial x_{AL}} = \frac{1}{y_R - y_L}$$

$$\frac{\partial V_6}{\partial x_{AL}} = \frac{-1}{y_R - y_L} S_F$$

Derivatives with respect to x_{AR}

$$\frac{\partial U_1}{\partial x_{AR}} = 0$$

$$\frac{\partial U_2}{\partial x_{AR}} = 0$$

$$\frac{\partial U_3}{\partial x_{AR}} = 0$$

$$\frac{\partial V_1}{\partial x_{AR}} = \frac{-y_L}{y_R - y_L} R_F \tag{8.10}$$

$$\frac{\partial V_2}{\partial x_{AR}} = \frac{y_L}{y_R - y_L}$$

$$\frac{\partial\ V_3}{\partial\ x_{AR}} = \frac{1}{y_R - y_L} R_F + \frac{-y_L}{y_R - y_L} S_F$$

$$\frac{\partial\ V_4}{\partial\ x_{AR}} = 0$$

$$\frac{\partial\ V_5}{\partial\ x_{AR}} = \frac{-1}{y_R - y_L}$$

$$\frac{\partial\ V_6}{\partial\ x_{AR}} = \frac{1}{y_R - y_L} S_F$$

Derivatives with respect to x_{FL}

$$\frac{\partial\ U_1}{\partial\ x_{FL}} = 0$$

$$\frac{\partial\ U_2}{\partial\ x_{FL}} = 0$$

$$\frac{\partial\ U_3}{\partial\ x_{FL}} = 0$$

$$\frac{\partial\ V_1}{\partial\ x_{FL}} = \frac{y_R}{y_R - y_L} R_A$$

$$\frac{\partial\ V_2}{\partial\ x_{FL}} = \frac{-y_R}{y_R - y_L} \tag{8.11}$$

$$\frac{\partial\ V_3}{\partial\ x_{FL}} = \frac{y_R}{y_R - y_L} S_A + \frac{-1}{y_R - y_L} R_A$$

$$\frac{\partial\ V_4}{\partial\ x_{FL}} = 0$$

$$\frac{\partial\ V_5}{\partial\ x_{FL}} = \frac{1}{y_R - y_L}$$

$$\frac{\partial\ V_6}{\partial\ x_{FL}} = \frac{-1}{y_R - y_L} S_A$$

Derivatives with respect to x_{FR}

$$\frac{\partial\ U_1}{\partial\ x_{FR}} = 0$$

$$\frac{\partial\ U_2}{\partial\ x_{FR}} = 0$$

$$\frac{\partial\ U_3}{\partial\ x_{FR}} = 0$$

$$\frac{\partial\ V_1}{\partial\ x_{FR}} = \frac{-y_L}{y_R - y_L} R_A$$

$$\frac{\partial\ V_2}{\partial\ x_{FR}} = \frac{y_L}{y_R - y_L} \tag{8.12}$$

$$\frac{\partial\ V_3}{\partial\ x_{FR}} = \frac{-y_L}{y_R - y_L} S_A + \frac{1}{y_R - y_L} R_A$$

$$\frac{\partial\ V_4}{\partial\ x_{FR}} = 0$$

$$\frac{\partial\ V_5}{\partial\ x_{FR}} = -\frac{1}{y_R - y_L}$$

$$\frac{\partial\ V_6}{\partial\ x_{FR}} = \frac{1}{y_R - y_L} S_A$$

The derivatives $\frac{\partial\ I_{TR}}{\partial\ x}$, where x is any shape variable, are prepared using Refs. 34 and 35. The shape sensitivities of the area integrals are linear combinations of other members of the same table of integrals. No new integrations are needed for the sensitivities.

With this information, the derivative of the mass term M_{rs} is calculated as follows:

$$\frac{\partial M_{rs}}{\partial\ x} = \rho_m \sum_{k=1}^{N_t} \overline{T}_k \sum_{i=1}^{3}\sum_{j=1}^{6}\sum_{ii=1}^{3}\sum_{jj=1}^{6} \left\{ \frac{\partial \left(U_i V_j U_{ii} V_{jj} \right)}{\partial x} I_{TR(m,n)} + U_i V_j U_{ii} V_{jj} \frac{\partial I_{TR(m,n)}}{\partial\ x} \right\} \tag{8.13}$$

with

$$m = m_j^v + m_{jj}^v + m_r^w + m_s^w + m_k^t$$

$$n = n_i^u + n_{ii}^u + n_j^v + n_{jj}^v + n_r^w + n_r^w + n_k^t$$

8.3 Stiffness Matrix Sensitivities

With the explicit expression of stiffness matrix elements in terms of thickness, fiber directions and shape of the panel available in Eq. 5.18, it is straightforward to obtain sensitivities analytically.

8.3.1 Stiffness Sensitivities With Respect to Thickness Design Variables T_k^i

Planform shape variables and orientation angles are fixed in this case. The thickness coefficients T_k^i appear in the expression for the stiffness matrix (Eq. 5.18) explicitly in a triple summation over the indices k, l1 and l2. Sensitivity is then obtained by direct differentiation, noting that if the design variable involved is T_r^q, then $\partial T_k^i / \partial T_r^q = 1$ only when i=q and k=r. Otherwise, the derivative is zero.

Differentiating Eq. 5.18 leads to:

$$\frac{\partial K_{rs}}{\partial T_r^q} = \sum_{a=1}^{3}\sum_{b=1}^{3}\sum_{ii=1}^{3}\sum_{jj=1}^{6}\sum_{iii=1}^{3}\sum_{jjj=1}^{6}\sum_{i=1}^{N_L}\sum_{i1=1}^{N_L}\sum_{i2=1}^{N_L}\sum_{k=1}^{N_i}\sum_{l1=1}^{N_{i1}}\sum_{l2=1}^{N_{i2}}\frac{1}{12}F_{ii,jj}^{a,r}F_{iii,jjj}^{b,s}\overline{\overline{Q}}_{a,b}(\theta_i)\cdot$$
$$\frac{\partial}{\partial T_r^q}\left\{T_k^i T_{l1}^{i1} T_{l2}^{i2}\right\}\iint x^{(m_{rs})}y^{(n_{rs})}dxdy \tag{8.14}$$

with

$$m_{rs} = mf_{ii,jj}^{a,r} + mf_{iii,jjj}^{b,s} + m_k^{t_i} + m_{l1}^{t_{i1}} + m_{l2}^{t_{i2}}$$
$$n_{rs} = nf_{ii,jj}^{a,r} + nf_{iii,jjj}^{b,s} + n_k^{t_i} + n_{l1}^{t_{i1}} + n_{l2}^{t_{i2}}$$

8.3.2 Stiffness Sensitivities With Respect to Fiber Direction θ_i

The angle represents the direction of fibers in the i-th layer, and the stiffness matrix K_{rs} depends on θ_i through elements of the matrix $\left[\overline{\overline{Q}}(\theta_i)\right]$ (Eq. 5.6). The derivative of each term in the stiffness matrix will be calculated in the following manner. In the summation (Eq. 5.18) over i=1 to N_L, all matrices $\left[\overline{\overline{Q}}(\theta_i)\right]$ are set to zero, except the matrix $\left[\overline{\overline{Q}}(\theta_i)\right]$ corresponding to the θ_i variable considered. This particular $\left[\overline{\overline{Q}}(\theta_i)\right]$ is replaced (in Eq. 5.18) by the following expression:

$$\frac{\partial \overline{\overline{Q}}(\theta_i)}{\partial \theta_i} = -2[Q_1]\cos 2\theta_i - 4[Q_2]\cos 4\theta_i + 2[Q_3]\sin 2\theta_i + 4[Q_4]\sin 4\theta_i \tag{8.15}$$

Equation 5.18 is , thus, used for the sensitivity of the stiffness term, with the derivative Eq. 8.15 replacing $\left[\overline{\overline{Q}}(\theta_i)\right]$.

8.3.3 Stiffness Sensitivities With Respect to Panel Planform Variables y_L, y_R, x_{FL}, x_{FR}, x_{AL} and x_{AR}

Thickness coefficients and orientation angles are held fixed. The terms Krs of the stiffness matrix depend on the shape through the matrix $[F_3]$ and the integrals $I_{TR(m,n)}$. If x is any planform design variable then:

$$\frac{\partial\ F_{ij}^{qp}}{\partial\ x} = \left(\frac{\partial\ U_i}{\partial\ x}V_j + U_i\frac{\partial\ V_j}{\partial\ x}\right) \cdot \text{(Integers from table 5.1)} \tag{8.16}$$

The derivatives of the U_i and V_j coefficients and the integrals $I_{TR(m,n)}$ are the same as for the mass matrix developed in section 8.2. With this information the derivatives of the stiffness matrix can be calculated as:

$$\frac{\partial \mathrm{K_{rs}}}{\partial \mathrm{x}} = \sum_{a=1}^{3}\sum_{b=1}^{3}\sum_{ii=1}^{3}\sum_{jj=1}^{6}\sum_{iii=1}^{3}\sum_{jjj=1}^{6}\sum_{i=1}^{N_L}\sum_{i1=1}^{N_L}\sum_{i2=1}^{N_L}\sum_{k=1}^{N_i}\sum_{l1=1}^{N_{i1}}\sum_{l2=1}^{N_{i2}}\frac{1}{12}\cdot$$

$$\left\{\left[\frac{\partial F_{ii,jj}^{a,r}}{\partial \mathrm{x}}F_{iii,jjj}^{b,s} + F_{ii,jj}^{a,r}\frac{\partial F_{iii,jjj}^{b,s}}{\partial \mathrm{x}}\right]\cdot \overline{\overline{Q}}_{a,b}(\theta_i)T_k^i \cdot T_{l1}^{i1}\cdot T_{l2}^{i2}\cdot I_{TR\,(\mathrm{m,n})}\right. \tag{8.17}$$

$$\left. + F_{ii,jj}^{a,r}\cdot F_{iii,jjj}^{b,s}\cdot \overline{\overline{Q}}_{a,b}(\theta_i)T_k^i \cdot T_{l1}^{i1}\cdot T_{l2}^{i2}\cdot \frac{\partial \mathrm{I_{TR\,(m,n)}}}{\partial \mathrm{x}}\right\}$$

8.4 Geometric Stiffness Matrix Sensitivities

Equation 6.24 gives the geometric stiffness matrix explicitly in terms of the thickness, fiber direction, and shape design variables.

8.4.1 Geometric Stiffness Sensitivities With Respect to Thickness Design Variables T_k^{it}

The design variable in this case is the k-th coefficient in the polynomial thickness series for the i-th layer. Examination of Eq. 6.24 reveals that the geometric stiffness matrix is explicitly linear in the

thickness coefficients T_k^{it}. It is, of course, also dependent on those coefficients via the wing box solution $\{\bar{q}\}$, unless it is assumed that in-plane loads [N] do not change. Differentiation of Eq. 6.24, using Eq. 33 leads to

$$\frac{\partial K_{G\,r,s}}{\partial T_k^{it}} = -\frac{1}{2}\sum_{a=1}^{2}\sum_{b=1}^{2}\sum_{i=1}^{3}\sum_{j=1}^{6}\sum_{ii=1}^{3}\sum_{jj=1}^{6}\sum_{ih=1}^{N_h}\sum_{qw=1}^{3}\sum_{pw=1}^{\overline{N}w}\sum_{R=1}^{N_L}\sum_{S=1}^{Nt_i}\tilde{F}_{2i,j}^{a,r}\cdot\tilde{F}_{2ii,jj}^{b,s}\cdot$$

$$\cdot\overline{\overline{Q}}_{ppp,qw}(\theta_{it})\cdot W_{qw,pw}\cdot H_{ih}[\Gamma_{k,S}^{it,R}\cdot\bar{q}_{pw}+T_S^R\cdot\frac{\partial\bar{q}_{pw}}{\partial T_k^{it}}]\cdot I_{TR}(mG_{r,s},nG_{r,s}) \quad (8.18)$$

where

$$mG_{r,s} = mf2_{i,j}^{a,r} + mf2_{ii,jj}^{b,s} + m_{ih} + mt_k^{it} + \tilde{m}_{qw,pw}$$

$$nG_{r,s} = nf2_{i,j}^{a,r} + nf2_{ii,jj}^{b,s} + n_{ih} + nt_k^{it} + \tilde{n}_{qw,pw}$$

and $\Gamma_{k,S}^{it,R}$ is equal to 1 only when it=R and k=S. Otherwise, it is zero.

8.4.2 Geometric Stiffness Sensitivities with Respect to Fiber Direction θ_{it}

Layer orientations affect the geometric stiffness matrix through the material matrices $\overline{\overline{Q}}_{ppp,qw}(\theta_{it})$ and the wing box generalized displacements $\{\bar{q}\}$. The analytic sensitivity with respect to fiber direction in a given layer is:

$$\frac{\partial K_{G\,r,s}}{\partial\theta_{it}} = -\frac{1}{2}\sum_{a=1}^{2}\sum_{b=1}^{2}\sum_{i=1}^{3}\sum_{j=1}^{6}\sum_{ii=1}^{3}\sum_{jj=1}^{6}\sum_{ih=1}^{N_h}\sum_{qw=1}^{3}\sum_{pw=1}^{\overline{N}w}\sum_{itt=1}^{N_L}\sum_{k=1}^{Nt_i}\tilde{F}_{2i,j}^{a,r}\tilde{F}_{2ii,jj}^{b,s}\cdot$$

$$[\frac{\partial\overline{\overline{Q}}_{ppp,qw}(\theta_{itt})}{\partial\theta_{it}}\bar{q}_{pw}+\overline{\overline{Q}}_{ppp,qw}(\theta_{itt})\frac{\partial\bar{q}_{pw}}{\partial\theta_{it}}]\cdot W_{qw,pw}H_{ih}T_k^{it}I_{TR}(mG_{r,s},nG_{r,s}) \quad (8.19)$$

Where the derivatives of $\overline{\overline{Q}}_{ppp,qw}(\theta_{it})$ are the same as for the stiffness matrix (Eq. 8.15)

8.4.3 Geometric Stiffness Sensitivities With Respect to Planform Variables y_L, y_R, x_{FL}, x_{FR}, x_{AL} and x_{AR}

Thickness coefficients and orientation angles are held fixed. The geometric stiffness matrix K_G depends on the planform variables through U_i and V_j terms in $\overline{F}{}_{2\,i,j}^{\,a,r}$ and $\overline{F}{}_{2\,ii,jj}^{\,b,s}$ (Table 6.2 and Eq. 6.24). There is also a dependence on the area integrals I_{TR} as discussed previously. The derivatives of the $[F_2]$ terms are calculated by:

$$\frac{\partial\ \overline{F}{}_{2ij}^{qp}}{\partial\ x} = \left(\frac{\partial\ U_i}{\partial\ x} V_j + U_i \frac{\partial\ V_j}{\partial\ x} \right) \cdot \text{(Integers from table 6.2)} \tag{8.20}$$

which is substituted into the derivative of K_G,

$$\frac{\partial\ K_{G\,r,s}}{\partial\ x} = -\frac{1}{2} \sum_{a=1}^{2} \sum_{b=1}^{2} \sum_{i=1}^{3} \sum_{j=1}^{6} \sum_{ii=1}^{3} \sum_{jj=1}^{6} \sum_{ih=1}^{N_h} \sum_{qw=1}^{3} \sum_{pw=1}^{\overline{N}w} \sum_{it=1}^{N_L} \sum_{k=1}^{Nt_i}$$

$$\left(\overline{\overline{Q}}_{ppp,qw}(\theta_{it}) \cdot W_{qw,pw} \cdot H_{ih} \cdot T_k^{it}\right) \cdot \left\{ \left(\frac{\partial\ \overline{F}{}_{2\,i,j}^{\,a,r}}{\partial\ x} \overline{F}{}_{2\,ii,jj}^{\,b,s} + \overline{F}{}_{2\,i,j}^{\,a,r} \frac{\partial\ \overline{F}{}_{2\,ii,jj}^{\,b,s}}{\partial\ x} \right) \cdot \bar{q}_{pw} I_{TR\,(\mathrm{m,n})} \right.$$

$$\left. + \overline{F}{}_{2\,i,j}^{\,a,r}\, \overline{F}{}_{2\,ii,jj}^{\,b,s} \cdot \left(\bar{q}_{pw} \frac{\partial\ I_{TR\,(\mathrm{m,n})}}{\partial\ x} + \frac{\partial\ \bar{q}_{pw}}{\partial\ x} I_{TR\,(\mathrm{m,n})} \right) \right\} \tag{8.21}$$

where the powers of integrands in $I_{TR(m,n)}$ are $m=mG_{r,s}$ and $n=nG_{r,s}$. In Eq. 8.21 it is assumed that overall wing planform is fixed, and panels are changing shape and location due to moving of control surfaces, ribs and spars. If overall planform shape of the wing is changing, then derivatives of the wing depth coefficients with respect to the shape design variables, $\partial H_{ih} / \partial x$, must be added, since the wing depth is defined in global x,y coordinates (Eq. 6.5).

When a constant in-plane load matrix is assumed using loads at a point (x_0,y_0) on the panel (Eqs. 6.27 and 6.28) then the motion of point (x_0,y_0) must be taken into account in the K_G shape sensitivity.

8.5 Aerodynamic Matrix Sensitivities

The aerodynamic stiffness and damping matrices are dependent only on the shape design variables through U_i and V_j and the integrals $I_{TR(m,n)}$. The sensitivities are obtained by direct differentiation of Eqs. 7.15 and 7.16.

$$\frac{\partial Q_{stiff\ rs}}{\partial \mathrm{x}} = \cos\phi \sum_{i=1}^{3}\sum_{j=1}^{6}\sum_{ii=1}^{3}\sum_{jj=1}^{6} \left\{ \frac{\partial\,(U_iV_jU_{ii}V_{jj})}{\partial x}(m_{jj}^{v}+m_{s}^{w})I_{TR\,(m-1,n)} + (U_iV_jU_{ii}V_{jj})(m_{jj}^{v}+m_{s}^{w})\frac{\partial I_{TR\,(m-1,n)}}{\partial \mathrm{x}} \right\} + \sin\phi \sum_{i=1}^{3}\sum_{j=1}^{6}\sum_{ii=1}^{3}\sum_{jj=1}^{6} \left\{ \frac{\partial\,(U_iV_jU_{ii}V_{jj})}{\partial x}(n_{ii}^{u}+n_{jj}^{v}+n_{s}^{w})I_{TR\,(m,n-1)} + (U_iV_jU_{ii}V_{jj})(n_{ii}^{u}+n_{jj}^{v}+n_{s}^{w})\frac{\partial I_{TR\,(m,n-1)}}{\partial \mathrm{x}} \right\} \tag{8.22}$$

$$\frac{\partial Q_{damp\ rs}}{\partial \mathrm{x}} = \sum_{i=1}^{3}\sum_{j=1}^{6}\sum_{ii=1}^{3}\sum_{jj=1}^{6} \left\{ \frac{\partial\,(U_iV_jU_{ii}V_{jj})}{\partial x}\cdot I_{TR\,(m,n)} + U_iV_jU_{ii}V_{jj}\frac{\partial I_{TR\,(m,n)}}{\partial x} \right\} \tag{8.23}$$

in both equations $m = (m_j^v + m_{jj}^v + m_r^w + m_s^w)$ and $n = (n_i^u + n_{ii}^u + n_j^v + n_{jj}^v + n_r^w + n_s^w)$

Recall from Eq. 7.17 that the coefficients relating A_{stiff} and A_{damp} to Q_{stiff} and Q_{damp} are functions of the Mach number only, which is held constant in this analysis (although sensitivities with respect to Mach number are easy to calculate). Therefore the sensitivities of A_{stiff} and A_{damp} are:

$$\begin{aligned} \frac{\partial A_{stiff}}{\partial \mathrm{DV}} &= \frac{1}{\sqrt{M_\infty^2-1}}\frac{\partial Q_{stiff}}{\partial \mathrm{DV}} \\ \frac{\partial A_{damp}}{\partial \mathrm{DV}} &= \frac{1}{\sqrt{M_\infty^2-1}}\frac{M_\infty^2-2}{M_\infty^2-1}\frac{\partial A_{dampf}}{\partial \mathrm{DV}} \end{aligned} \tag{8.24}$$

8.6 More on the Analytical Sensitivities

It is clear, examining the analytic sensitivities of the system matrices derived in the previous sections, that all involve area integrals of polynomial terms over the panel's area. Since members of the family of integrals $I_{TR}(m,n)$ are generated for the analysis stage, there is no need to generate them again for the sensitivity calculation stage. No numerical integration is therefore needed for either analysis or

sensitivity calculations. This is similar to the process by which analytic sensitivities are obtained for the wing box analysis (Refs. 34 and 35). A table of area integrals over the wing surface has to be generated once (using the same analytic formulas used here for the panel). The integrals are subsequently used for wing box analysis and sensitivities.

Of course, when the wing changes shape, panels change shape too. There is linking, therefore, between overall wing planform design variables and panel vertex locations. This linking has to be accounted for in the sensitivity computations when overall wing / panel shapes are changing.

8.7 Eigenvalue Sensitivities

The panel flutter problem was shown in Chapter 2 to be a generalized eigenvalue problem of the form:

$$\left[\overline{\overline{U}}\right]\{\phi\} = \lambda \left[\overline{\overline{V}}\right]\{\phi\} \tag{8.25}$$

Let the left eigenvectors be $\{\psi\}$ from the adjoint eigenvalue problem:

$$\{\psi\}^T\left[\overline{\overline{U}}\right] = \lambda \{\psi\}^T\left[\overline{\overline{V}}\right] \tag{8.26}$$

Recall that the matrices $\left[\overline{\overline{U}}\right]$ and $\left[\overline{\overline{V}}\right]$ are made up of the mass, aerodynamic, stiffness, and geometric stiffness matrices (Eqs. 2.41 and 2.45).

The sensitivity of the eigenvalues with respect to any design variable, DV, is obtained by differentiating Eq. 8.25:

$$\frac{\partial \left[\overline{\overline{U}}\right]}{\partial DV}\{\phi\} + \left[\overline{\overline{U}}\right]\frac{\partial \{\phi\}}{\partial DV} = \frac{\partial \lambda}{\partial DV}\left[\overline{\overline{V}}\right]\{\phi\} + \lambda\frac{\partial \left[\overline{\overline{V}}\right]}{\partial DV}\{\phi\} + \lambda\left[\overline{\overline{V}}\right]\frac{\partial \{\phi\}}{\partial DV} \tag{8.27}$$

Premultiplying by $\{\psi\}^T$ gives:

$$\{\psi\}^T\left[\frac{\partial \left[\overline{\overline{U}}\right]}{\partial DV} - \lambda\frac{\partial \left[\overline{\overline{V}}\right]}{\partial DV}\right]\{\phi\} + \{\psi\}^T\left[\left[\overline{\overline{U}}\right] - \lambda\left[\overline{\overline{V}}\right]\right]\frac{\partial \{\phi\}}{\partial DV} = \frac{\partial \lambda}{\partial DV}\{\psi\}^T\left[\overline{\overline{V}}\right]\{\phi\} \tag{8.28}$$

From 8.26 the second term is zero leaving:

$$\frac{\partial \lambda}{\partial \mathrm{DV}} = \frac{\{\psi\}^T \left[\frac{\partial \left[\overline{\overline{U}}\right]}{\partial DV} - \lambda \frac{\partial \left[\overline{\overline{V}}\right]}{\partial DV} \right] \{\phi\}}{\{\psi\}^T \left[\overline{\overline{V}}\right] \{\phi\}} \tag{8.29}$$

The derivatives of $\left[\overline{\overline{U}}\right]$ and $\left[\overline{\overline{V}}\right]$ are obtained using the sensitivities of all of the system matrices:

$$\frac{\partial \left[\overline{\overline{U}}\right]}{\partial DV} = \left[\begin{array}{c|c} 0 & 0 \\ \hline -\frac{\partial \left[\overline{\overline{K}}\right]}{\partial DV} & -\frac{\partial \left[\overline{\overline{C}}\right]}{\partial DV} \end{array} \right]$$

$$\frac{\partial \left[\overline{\overline{V}}\right]}{\partial DV} = \left[\begin{array}{c|c} 0 & 0 \\ \hline 0 & \frac{\partial \left[\overline{\overline{M}}\right]}{\partial \mathrm{DV}} \end{array} \right] \tag{8.30}$$

where

$$\frac{\partial \overline{\overline{M}}}{\partial \mathrm{DV}} = \frac{\partial M}{\partial \mathrm{DV}}$$

$$\frac{\partial \overline{\overline{C}}}{\partial \mathrm{DV}} = -\rho_\infty U_\infty \frac{\partial A_{damp}}{\partial \mathrm{DV}} \tag{8.31}$$

$$\frac{\partial \overline{\overline{K}}}{\partial \mathrm{DV}} = \frac{\partial \mathrm{K}}{\partial \mathrm{DV}} + \frac{\partial \mathrm{K_G}}{\partial \mathrm{DV}} - \rho_\infty U_\infty^2 \frac{\partial A_{stiff}}{\partial \mathrm{DV}}$$

Therefore, we can calculate the eigenvalue sensitivities directly from the eigenvectors, eigenvalues, and the individual matrix sensitivities. The eigenvalue sensitivities are useful to the designer because the real part of the sensitivity will show the rate at which a particular root is going towards the right-half s-plane indicating how quickly that root is nearing instability.

A more useful piece of information, however, is the sensitivity of the flutter dynamic pressure itself. If we look at the real part of an eigenvalue, σ, and allow the design variable and dynamic pressure to change then we have $\sigma = \sigma(q_{flutter}, DV)$. At the flutter dynamic pressure, the real part of the root is zero by definition of the flutter point. A variation of σ at flutter is then given as:

$$\partial \sigma = \frac{\partial \sigma}{\partial \mathrm{DV}} \partial DV + \frac{\partial \sigma}{\partial \mathrm{q}_{\mathrm{flutter}}} \partial q_{flutter} = 0 \tag{8.32}$$

which can be rearranged to give the sensitivity of the flutter dynamic pressure as:

$$\frac{\partial q_{flutter}}{\partial \mathrm{DV}} = \frac{-\dfrac{\partial \sigma}{\partial \mathrm{DV}}}{\dfrac{\partial \sigma}{\partial \mathrm{q}_{\mathrm{flutter}}}} = \frac{-\mathrm{Re}\left(\dfrac{\partial \lambda}{\partial \mathrm{DV}}\right)}{\mathrm{Re}\left(\dfrac{\partial \lambda}{\partial \mathrm{q}_{\mathrm{flutter}}}\right)} \tag{8.33}$$

The numerator is known already from Eq. 8.29. The denominator is found by replacing DV with $q_{flutter}$ in Eq. 8.29 where

$$\begin{gathered}\frac{\partial \left[\overline{\overline{U}}\right]}{\partial q_{flutter}} = \left[\begin{array}{c|c} 0 & 0 \\ \hline -2\left[A_{stiff}\right] & -\dfrac{2}{U_\infty}\left[A_{damp}\right] \end{array}\right] \\ \frac{\partial \left[\overline{\overline{V}}\right]}{\partial q_{flutter}} = [0] \end{gathered} \tag{8.34}$$

The sensitivity of the flutter dynamic pressure with respect to the design variables tells the designer where the stability boundary will move if a design variable is changed. The sensitivity can also be used to construct approximations for optimization based on approximation concepts (Ref. 39). A final note on the flutter sensitivity equation (Eq. 8.33): some special cases may be encountered when multiple roots with non-distinct eigenvalues appear in the stability analysis. These cases are beyond the scope of this work, and more information can be found in Refs. 40 and 41.

CHAPTER 9

VERIFICATION OF RESULTS

9.1 Introduction

The numerical results of the computer code implementing the techniques described in this work are compared with data from the panel flutter literature to verify its capabilities. First the convergence of the solution for increasing orders of Ritz polynomials is shown to establish the number of terms necessary for accurate results. Then results are presented for configurations of increasing complexity and compared with available data. The capability to accurately predict flutter boundaries is shown for simply supported skewed and trapezoidal shapes, yawed flow, variable composite fiber orientations, in-plane loads, and combinations of the above. The analytic sensitivities are compared with finite difference approximations for validation. Finally, the capability of the code to use analytic sensitivities for direct and reciprocal approximations of flutter boundaries is demonstrated.

All of the isotropic test cases use aluminum material properties of $E = 6.8959 \times 10^{10}$ Pa, $\rho_m = 2768\ kg_{mass}/m^3$, and a poisson's ratio of 0.3. All of the composite test cases use the material properties of $E_1=137 \times 10^9$ Pa, $E_2=9.7 \times 10^9$ Pa, $G_{12}=5.5 \times 10^9$ Pa, $\rho_m=1580\ kg_{mass}/m^3$, and $\upsilon_{12}=0.3$.

9.2 Convergence to Solution

Results are compared with Refs. 5 and 23 to show the convergence rate of the present analysis. The panels chosen from Ref. 5 are a square and rectangular isotropic aluminum panel (Fig. 9.2). The panel in Ref. 23 is a 45° skewed panel made up of a single layer composite with a fiber angle of 15° (Fig. 9.4). Figure 9.1 shows that satisfactory convergence is obtained with either a fourth or fifth order polynomial Ritz series (Eq. 3.8). While the computational time is significantly reduced by using a fourth order polynomial, Figure 9.1 shows an example of a panel that requires a fifth order polynomial. Most panel configurations converged with fourth order series, but because of the exceptions, a fifth order approximation is needed. Therefore all of the results presented here are based on a fifth order Ritz polynomial.

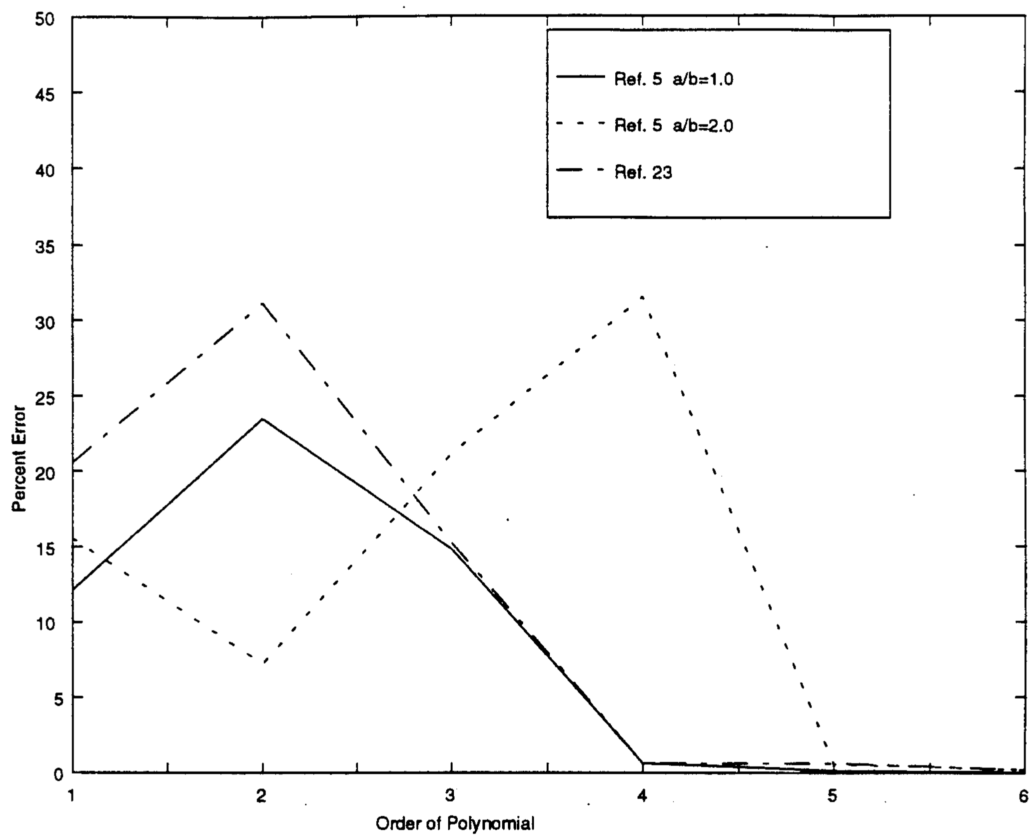

Figure 9.1 Convergence of Solution for Critical Dynamic Pressure with no In-Plane Loads

9.3 Isotropic Rectangular Panels in Yawed Flow

Results are compared with the analytical and FEM data of Ref. 5 to show the effects of yawed flow and rectangular aspect ratios. An aluminum plate was used with the following geometry.

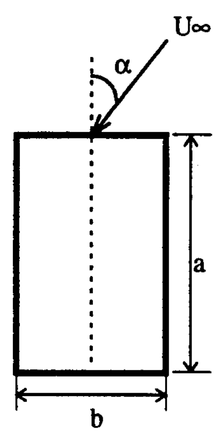

Figure 9.2 Panel Geometry for Ref. 5

Reference 5 defines the flow angle differently than the present analysis (Figure 7.1). The relation is $\alpha = -\phi$. The panel width, b, is held constant at 1.0m and panel thickness, h, is varied from 2 mm to 5 mm so that the panel flutters at a meaningful dynamic pressure. The Mach number is held constant at 2.0. The results are given as a non-dimensional critical dynamic pressure,

$$\Lambda_{crit} = \frac{2q_{crit}\, a^3}{D\sqrt{M^2 - 1}} \tag{9.1}$$

Table 9.1 Λ_{crit} for Rectangular Isotropic Panels

(No In-Plane Loads)

a/b	Model	$\alpha = 0°$	$\alpha = 30°$	$\alpha = 45°$
0.5	Analytical	385.0	—	—
	Sander	382.0	213.0	172.0
	Present	383.2	214.9	175.5
1.0	Analytical	512.6	—	—
	Sander	503.0	516.0	523.0
	Present	511.9	527.0	530.7
1.25	Analytical	615.0	—	—
	Sander	612.6	—	—
	Present	614.1	658	712
2.0	Analytical	1110	—	—
	Sander	1081	1206	1388
	Present	1106	1201	1415

Table 9.1 summarizes the results. It shows that the present technique compares well with both the analytical and FEM results of Ref. 5 for variable aspect ratios and yaw angles.

9.4 Isotropic Skewed Panels Subjected to In-Plane Loads

We show the effects of skewed panels, yawed flow, and in-plane forces by comparing data with the FEM results of Ref. 21. Here we use a simply supported aluminum panel with h = 2mm and $M_\infty = 2.0$. The geometry is defined in Fig. 9.3.

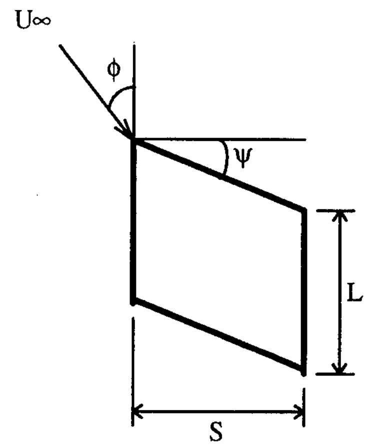

Figure 9.3 Panel Geometry for Ref. 21

The results are given in the same non-dimensional dynamic pressure:

$$\Lambda_{crit} = \frac{2q_{crit}\, L^3}{D\sqrt{M^2 - 1}} \tag{9.2}$$

Table 9.2 shows results for a flow angle of $\phi = 0°$ and Table 9.3 shows the same configurations with $\phi = 15°$. The present results do not agree with Ref. 21 very well for some of the configurations. Recall from Chapter 2 that q_{crit} is found by ignoring damping and looking for a coalescence of eigenvalues. In most cases the coalescence frequency is between the first and second or second and third frequencies. However, in the cases marked by ** our results showed a coalescence of the 14th and 15th roots before the first and second roots. The cases marked * had a coalescence of the fifth and sixth roots before the first and second roots. The results of such cases are shown as the first and second frequency coalescence followed by the higher pole coalescence.

Table 9.2 Λ_{crit} for Skewed Panels with $\phi = 0°$

L/S	Model	$\psi = 0°$	$\psi = 15°$	$\psi = 30°$
0.5	Ref. 21	374.1	303.9	325.3
	Present	383.4	**289/50.7	242.4
1.0	Ref. 21	518.2	548.4	668.2
	Present	511.9	518.0	522.0
2.0	Ref. 21	1147	1247	1500
	Present	1106	*1118/622	1138

Table 9.3 Λ_{crit} for Skewed Panels with $\phi = 15°$

L/S	Model	$\psi = 0°$	$\psi = 15°$	$\psi = 30°$
0.5	Ref. 21	292.2	222.1	243.5
	Present	274.7	**222/195	193.9
1.0	Ref. 21	521.1	487.0	579.6
	Present	515.1	501.4	482.6
2.0	Ref. 21	1188	1169	1948
	Present	1134	*1149/656	1167

The cases marked by * and ** in Tables 9.2 and 9.3 were re-computed with aerodynamic damping for comparison. With the damping, the same higher order poles converged, but there was enough damping to keep them stable. Therefore, the model with damping converged to flutter boundaries in better agreement with Ref. 21. These additional test cases are shown in Table 9.4. Reference 30 discusses cases involving modes of nearly identical frequencies, but weak aerodynamic coupling, that lead to inaccurate results in the abscence of aerodynamic damping. This may be occuring in these cases and should be further investigated.

Table 9.4 $\Lambda_{flutter}$ and Λ_{crit} for Skewed Panels

		$\psi = 15°$	
L/S	Model	ϕ=0°	ϕ=15°
0.5	Ref. 21 Λ_{crit}	303.9	221.1
	Present Λ_{flutt}	306.3	229.7
2.0	Ref. 21 Λ_{crit}	1247	1169
	Present Λ_{flutt}	1135	1168

Finally we compare results with in-plane forces. Reference 21 uses a non-dimensional in-plane force that can be defined as:

$$r_{ij} = \frac{N_{ij}\ L^2}{\pi^2 D} \tag{9.3}$$

The results are for a square panel (L/S=1) with $\phi = 0°$.

Table 9.5 Critical Dynamic Pressures With $r_{yy} = r_{xy} = 0$

Model	$r_{xx} = -3$	$r_{xx} = 0$	$r_{xx} = 3$
Ref. 21	275.7	518.2	789.0
Present	265.1	512.6	793.1

Table 9.6 Critical Dynamic Pressures With $r_{xx} = r_{yy} = 0$

Model	$r_{xy} = 0$	$r_{xy} = 2$	$r_{xy} = 4$	$r_{xy} = 6$
Ref. 21	518.2	487.0	418.9	321.5
Present	512.6	473.1	381.7	274.3

Note the expected decrease in critical dynamic pressure with increasing axial compression or in-plane shear.

9.5 Skewed Composite Panels

To show the effects of skew angle and composite fiber angle, results were compared with Ref. 23. The geometry is defined in Fig. 9.4.

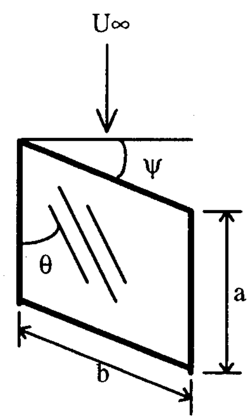

Figure 9.4 Panel Geometry for Ref. 23

Table 9.7 compares the results for the case of an isotropic aluminum panel with a=b=1.0m, h=3mm and M_∞=2.0. The results are in terms of the nondimensional critical dynamic pressure:

$$\Lambda_{crit} = \frac{2q_{crit}\, a^3}{D\sqrt{M^2 - 1}} \tag{9.4}$$

Table 9.7 Λ_{crit} for Various Skew Angles

	$\psi = 0°$	$\psi = 15°$	$\psi = 30°$
Ref. 23	511	522	664
Presnt	513	532	606/347*

With a skew angle of 30° the fifth and sixth poles coalesced at the lower dynamic pressure, however this did not occur with aerodynamic damping.

Table 9.8 shows the critical dynamic pressure for composite panels with various fiber and skew angles. Table 9.9 shows the corresponding critical frequencies. The results are non-dimensionalized as:

$$\Lambda_{crit} = \frac{2q_{crit}\, a^3}{E_2 h^3 \sqrt{M^2 - 1}} \tag{9.5}$$

$$\Omega_{cr} = \omega_{cr}\, a^2 \sqrt{\frac{\rho_m}{E_2 h^2}} \tag{9.6}$$

The composite panel used had a=b=1 m and h=4 mm.

Table 9.8 Λ_{crit} for Skewed Composite Panel

	ψ=15°		ψ=30°		ψ=45°	
θ	Λ_{cr} Ref. 23	Λ_{cr} Present	Λ_{cr} Ref. 23	Λ_{cr} Present	Λ_{cr} Ref. 23	Λ_{cr} Present
0°	358	387	367	389	427	*429/104
15°	248	246	299	301	321	319
30°	170	163	202	195	257	254
45°	120	116	138	133	183	180
60°	81	79.5	92	88.5	160	128
75°	60	57.5	87	73.1	188	135
90°	69	57.4	124	81.8	238	164

Table 9.9 Ω_{crit} for Skewed Composite Panels

	ψ=15°		ψ=30°		ψ=45°	
θ	Ω_{cr} Ref. 23	Ω_{cr} Present	Ω_{cr} Ref. 23	Ω_{cr} Present	Ω_{cr} Ref. 23	Ω_{cr} Present
0°	28.4	30.4	29.3	30.9	34.4	*34.7/53.3
15°	24.3	24.7	30.3	31.1	32.6	33.1
30°	23.4	23.5	26.6	27.0	30.7	31.7
45°	22.0	22.0	23.0	23.6	28.4	28.6
60°	19.3	19.4	21.0	21.0	30.3	28.7
75°	17.9	17.9	22.5	21.8	35.8	33.5
90°	19.3	18.9	26.6	24.6	41.7	39.0

The case marked by * had a coalescence of the third and fourth frequencies before the first and second. However, the results for most of the above configurations are very close to Ref. 23. As skew angle and fiber angle increase, correlation of the present results and Ref. 23 deteriorates. Notice that the above geometries are very close to the geometries of the skewed panels in Ref. 21 but the results compare much more favorably.

Data for the flutter dynamic pressures and frequencies (aerodynamic damping present) was also obtained for these test cases and is shown in Table 9.10. The addition of the aerodynamic damping changed the predicted stability boundaries by only a few percent and the results are very close to Ref. 23. As before, with aerodynamic damping, any higher frequencies that coalesced remained stable and the solution converged to an appropriate Λ_{flutt}.

Table 9.10 $\Lambda_{flutter}$ and $\Omega_{flutter}$ for Skewed Composite Panels

	ψ=15°		ψ=30°		ψ=45°	
θ	Λ_f Present	Ω_f Present	Λ_f Present	Ω_f Present	Λ_f Present	Ω_f Present
0°	449	36.8	439	34.1	447	35.5
15°	268	26.1	307	32.0	324	32.2
30°	166	23.6	198	27.1	257	31.8
45°	117	22.0	134	23.6	181	28.7
60°	80	19.4	89.2	21.0	129	28.7
75°	57.8	17.9	73.5	21.8	135	33.5
90°	57.7	18.9	82.3	24.6	165	39.0

The results are presented in graphical form in Figs. 9.5 and 9.6. The present results show the same effect of fiber angle on critical dynamic pressures as Ref. 23.

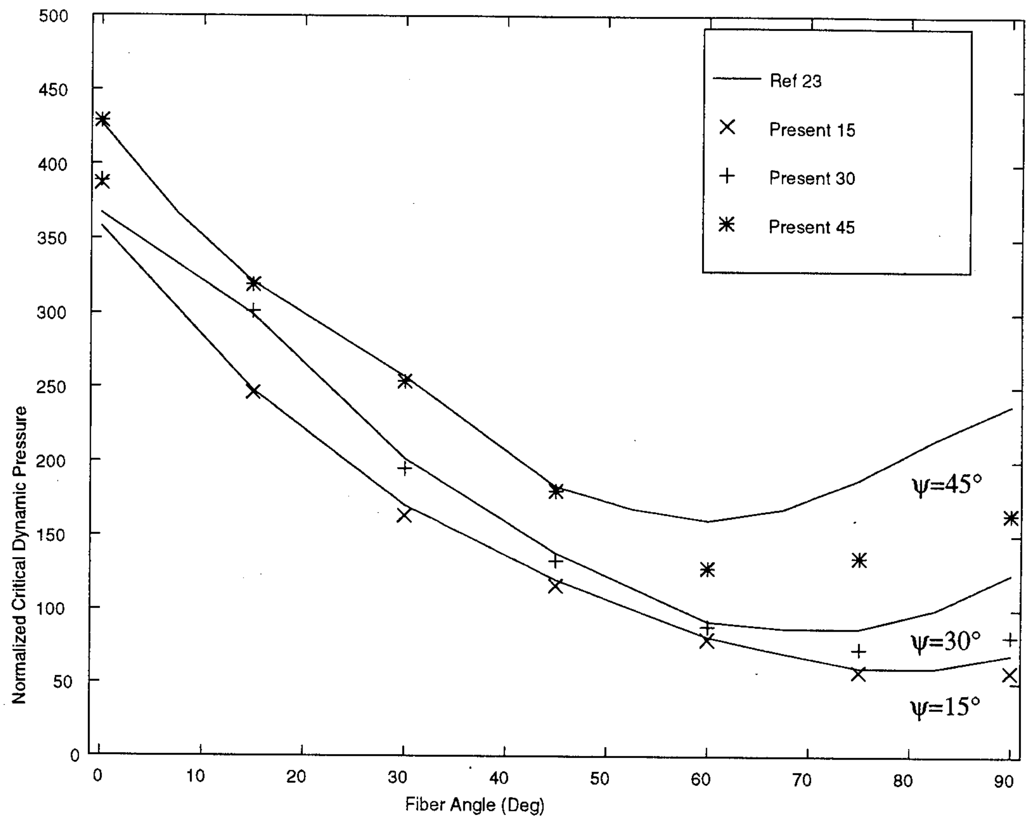

Fig. 9.5 Λ_{crit} versus Fiber Angle for Different Skew Angles

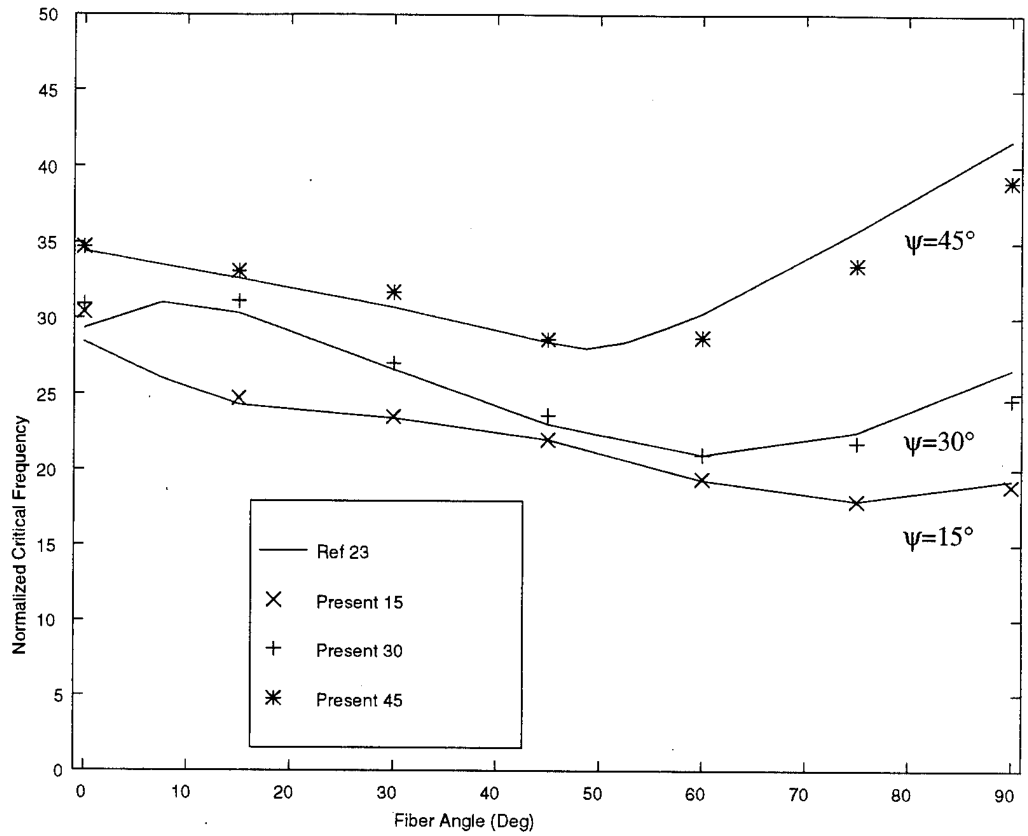

Fig. 9.6 Ω_{crit} versus Fiber Angle for Different Skew Angles

The present analysis shows the same effects of fiber angle on the critical pressure and frequency as Ref. 23. Overall, except in cases of high skew angle (45°) and high fiber angle, the results obtained here are in good correlation with the references.

9.6 Analytic Sensitivities

This section shows the accuracy of the analytic sensitivities and demonstrates some of the capabilities that they give the designer. Figure 9.7 shows the accuracy of the analytic fiber angle sensitivity compared with a finite difference approximation for a range of step sizes. The plot is based on the composite panel geometry shown in Fig 9.4 with ψ=15°, θ=45°,and a=b=1.0m. For a step size between 10^{-6} and 10^{-2} the finite difference and analytic sensitivities are nearly identical. A smaller step size results in an inaccurate finite difference estimate because of round off errors.

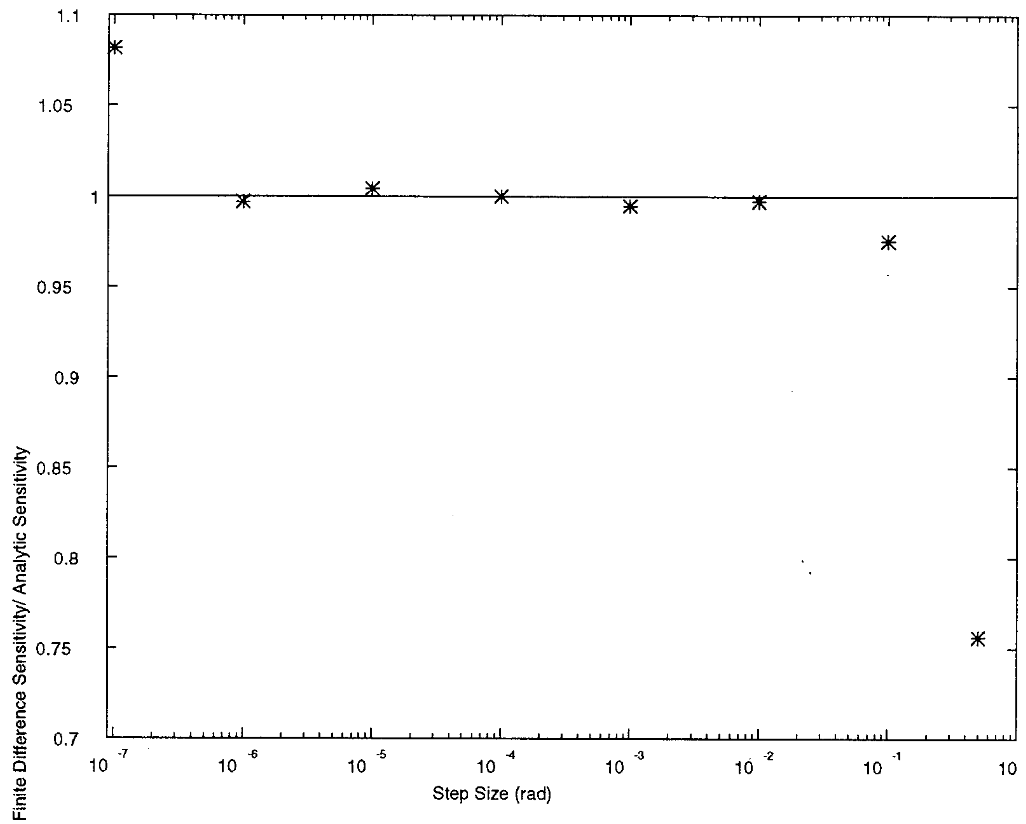

Fig. 9.7 Fiber Angle Sensitivity vs. Step Size

Table 9.11 compares the analytic sensitivities of skewed composite panels (Fig. 9.4) at θ=45° with finite difference approximations based on a step size of 10^{-4}.

Table 9.11 Fiber Angle Sensitivities at θ=45°

	$\psi = 0°$	$\psi = 15°$
$\frac{\partial \Lambda_{crit}}{\partial \theta}$	-153.0	-300.2
Finite Diff.	-153.0	-300.7
$\frac{\partial \Lambda_{flutt}}{\partial \theta}$	-155.8	-305.7
Finite Diff.	-155.8	-306.2

The analytic sensitivities above and the corresponding dynamic pressures are used to predict the effect of fiber angle on the stability boundary that was shown in secton 9.5. Figures 9.8 through 9.11 show the Taylor series and reciprocal approximations (Ref. 39). These approximations, both with and without aerodynamic damping, are good for a range of θ at least $\pm 15°$.

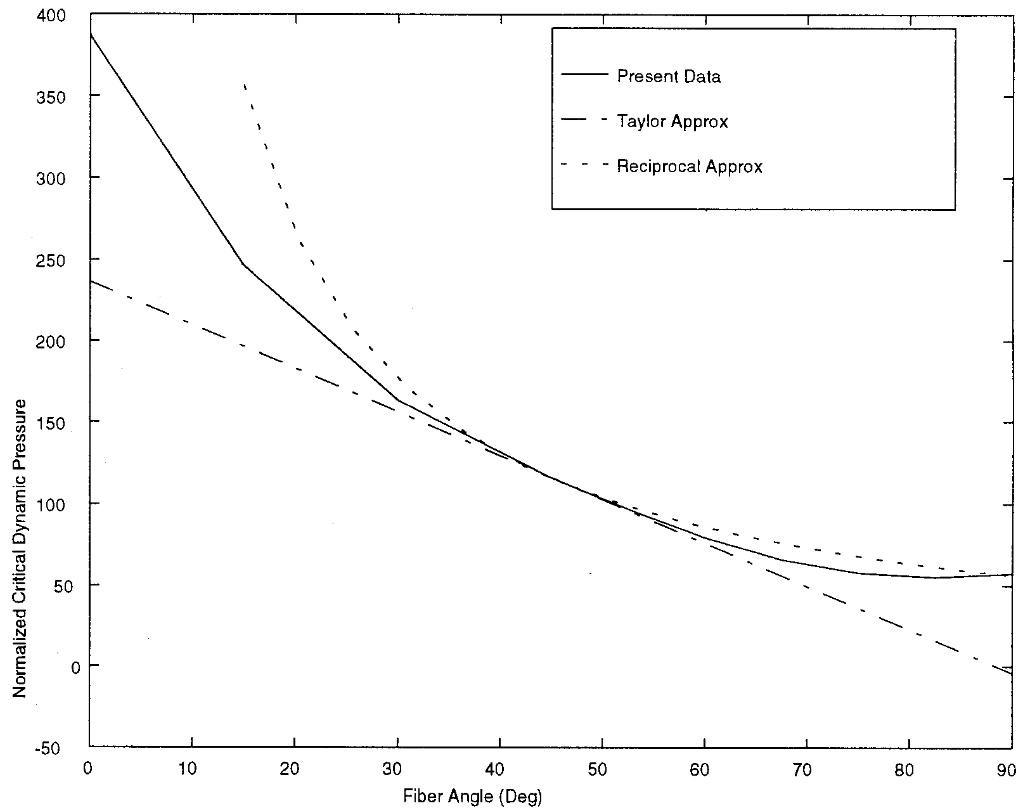

Figure 9.8 Λ_{crit} vs. Fiber Angle for ψ=15°

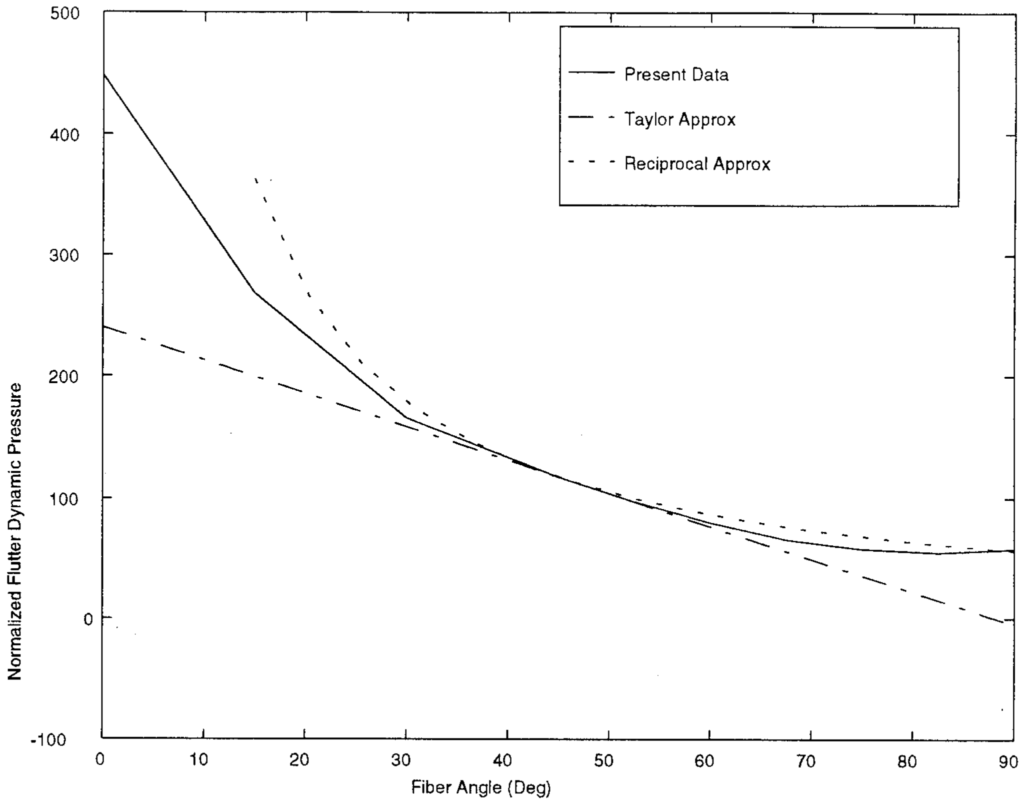

Figure 9.9 Λ_{flutt} vs. Fiber Angle for ψ=15°

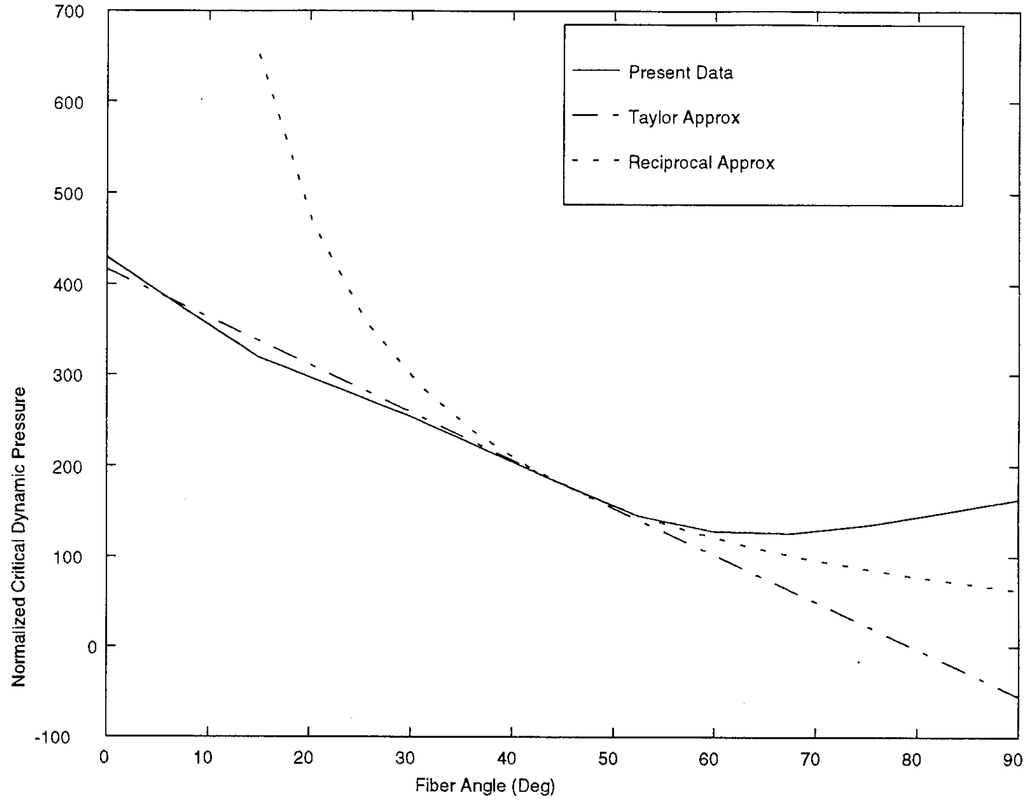

Figure 9.10 Λ_{crit} vs. Fiber Angle for ψ=45°

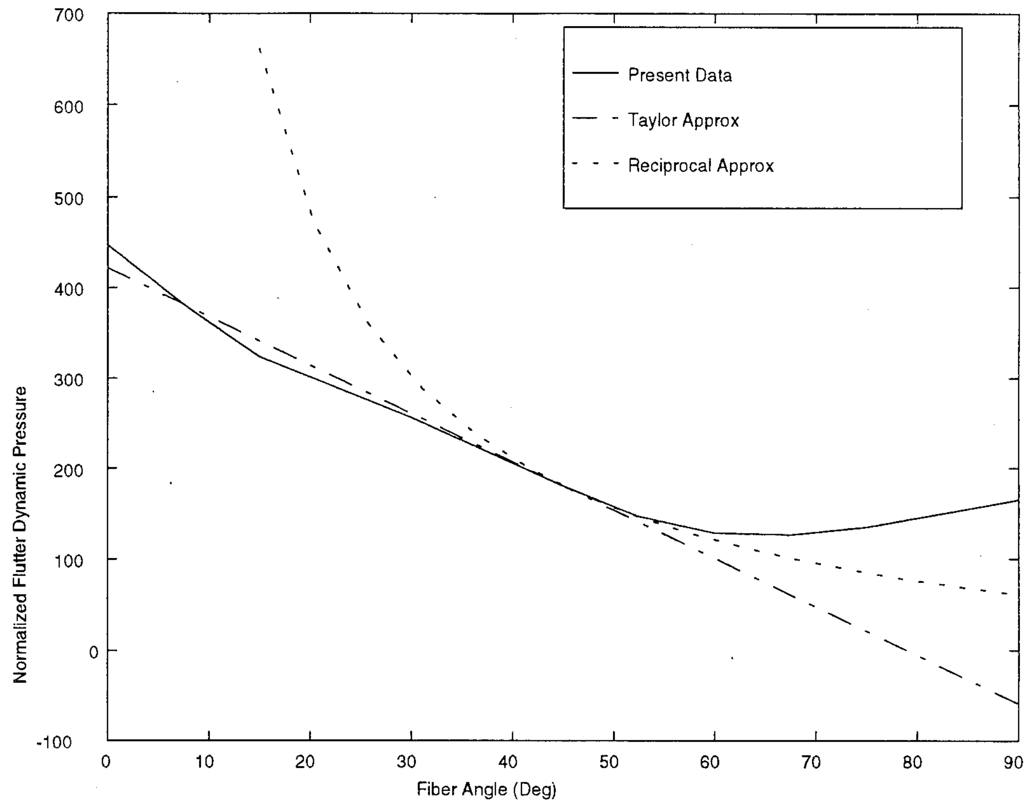

Figure 9.11 Λ_{flutt} vs. Fiber Angle for ψ=45°

To show the capabilities of the shape sensitivities we use X_{AR} as an example. A composite panel with ψ=30°, θ=15°, a=b=1.0m, and h=3mm was used as the referenc panel. X_{AR} was varied from 0.5 to 2.5 m to range from a triangular to trapezoidal panel as shown below.

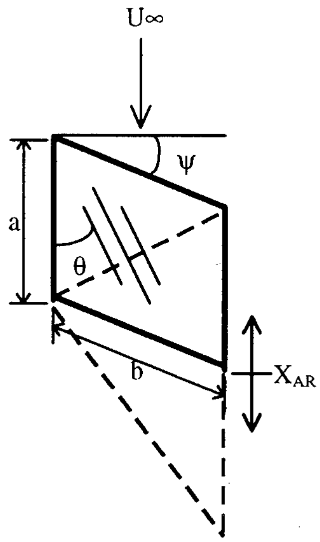

Figure 9.12 Panel Geometry For X_{AR} Sensitivity

Aerodynamic damping was included for this test case. The flutter dynamic pressure was normalized as:

$$\Lambda_{flutt} = \frac{2q_{\text{flutt}}\,a^3}{E_2 h^3 \sqrt{M^2 - 1}} \tag{9.7}$$

At X_{AR}=1.5m the analytic sensitivity was computed to be $\frac{\partial \Lambda_{\text{flutt}}}{\partial X_{\text{AR}}} = -415.9$. Figure 9.13 shows that both the first order Taylor series approximation and the reciprocal approximation give a good estimation of the affect of X_{AR} on the flutter boundary.

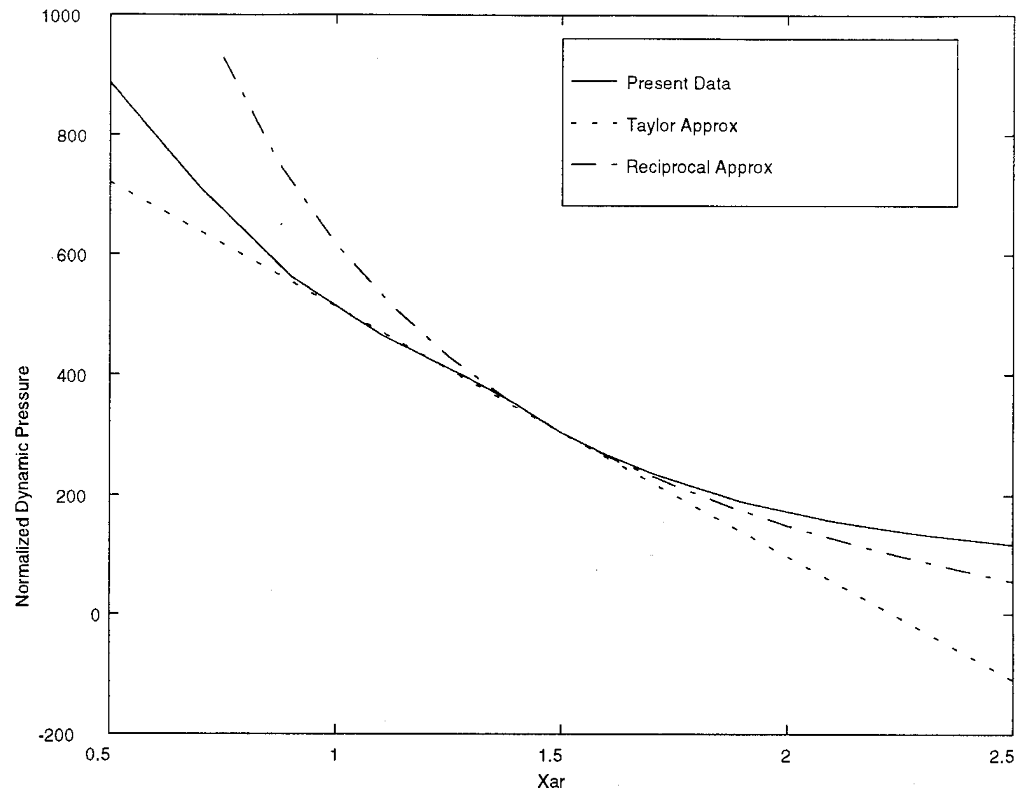

Figure 9.13 Λ_{flut} vs. Xar

Finally, we demonstrate the capability of predicting the effect of changing in-plane loads on the flutter boundary. Recall that the in-plane load matrix, [N], affects the equations of motion linearly through $[K_G]$. Therefore, we can keep the ratio of the N_{ij}'s the same but allow for changing magnitudes by simply multiplying $[K_G]$ by a factor, η. We used an isotropic panel defined by the geometry in Figure 9.4 with ψ=30°, a=b=1m, and h=3mm. The in-plane loads were applied as N_x= -2000, N_y= -1000, and N_{xy}=0. The load factor was varied from -5.0 to 3.0 to range over tension and compression up to the buckling point. The sensitivity was computed at η=1.0 to be $\dfrac{\partial \Lambda_{flutt}}{\partial \eta} = -99.99$.

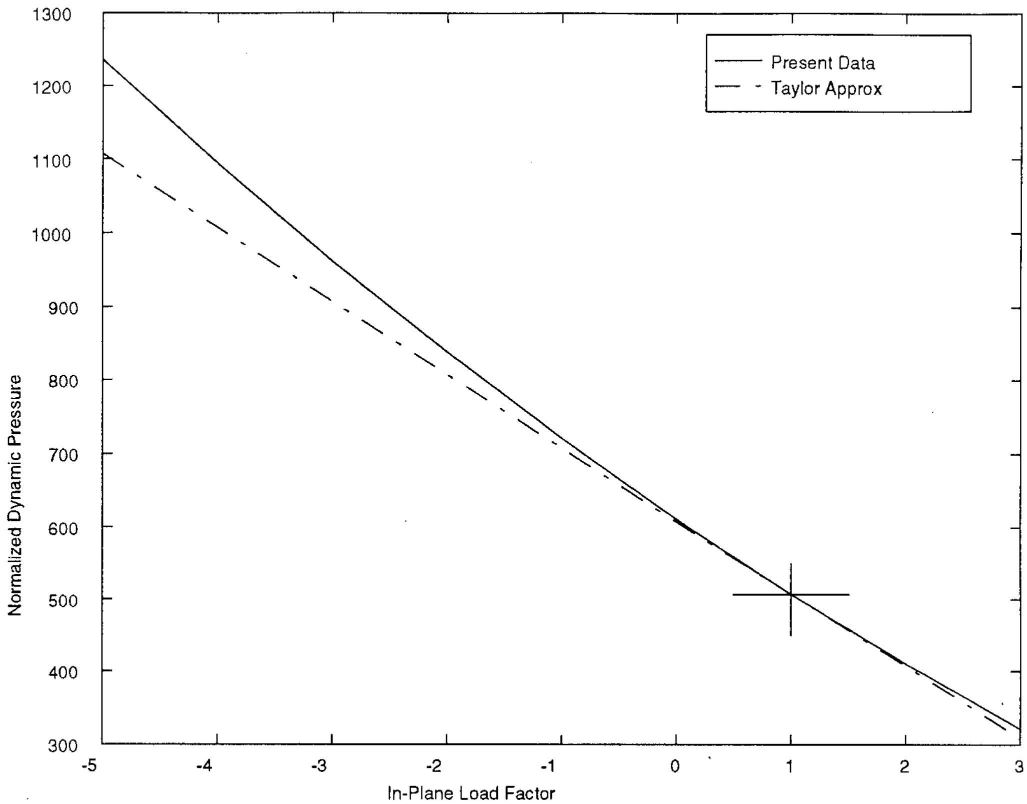

Figure 9.14 Λ_{flutt} vs. In-plane Load Factor, η

The present technique gives results in agreement with the available literature for a wide range of panel variables. The analytic sensitivities are very accurate when compared with finite difference approximations, and they have been shown to successfully predict the effects of changing shape, fiber angles, and in-plane loads.

CHAPTER 10

CONCLUSION

The capability to include configuration shape design variables, in any multidisciplinary design optimization of airplanes in the conceptual or preliminary design stages, is essential. Developments in recent years advanced the state of the art in Design Oriented Structural Analysis (DOSA) covering approximate stress, deformation, structural dynamic and buckling analysis as well as analytical behavior sensitivity techniques, where wing box structures, and skin panel structures, are subject to shape as well as material and sizing variations. The present work has focused on the design oriented aeroelastic analysis of optimized skin panels in supersonic flow. Since, in typical optimum aeroelastic synthesis of wing structures, many skin panels can be buckling-critical, and since stressing a panel up to a point close to its buckling load may have a serious effect on its aeroelastic stability as a panel, it becomes important to develop efficient analysis and sensitivity capabilities for panel flutter constraints.

It is shown in this work how modeling and Ritz formulations based on simple polynomial functions in global coordinates, lead to efficient evaluation of panel stiffness, geometric stiffness, and mass, as well as aerodynamic damping and aerodynamic stiffness matrices. Using analytic formulas for area integrals of polynomial terms over general trapezoidal area shapes, it is shown that no numerical integration is needed for evaluating panel structural or aerodynamic matrices. A table of area integrals for the panel, including area integrals over the panel of terms of the form $x^m \cdot y^n$, needs to be evaluated only once for a given panel shape. Then, structural and aerodynamic matrices, as well as their analytic sensitivities with respect to sizing, material and shape design variables, can be obtained by linear combinations of elements of this table of integrals.

Systematic evaluation of the resulting panel flutter prediction capability was carried out, comparing results from the present work with results from other references. Cases involving rectangular and skewed panels, isotropic and composite construction, and different types of in-plane loads were covered. Overall, the current capability led to good correlation with other prediction techniques up to panel leading edge sweep angles of 30°. Large differences in panel flutter boundary predictions between the current technique and other approximate techniques including finite elements, were observed for panel sweep angles of more than 30°. Additional work is needed in this area to find out whether the discrepancies are due to limitations of the current polynomial Ritz analysis or the other approximate and finite element techniques used for comparison. Unfortunately, only a few papers on panel flutter address the aeroelastic stability of panels of general trapezoidal shapes.

Expressions for analytic sensitivity of panel aeroelastic poles and resulting flutter dynamic pressure, have been obtained, and checked against finite difference sensitivities. Excellent correlation, and

a wide range of step sizes for the finite difference derivatives, have been found. Used, in turn, in direct and reciprocal Taylor series approximations for the flutter dynamic pressure, the flutter and sensitivity results have been shown to lead to quite robust approximations over a wide range of design variable changes (wide move limits). The work has also shown how to integrate the panel aeroelastic analysis and sensitivity predictions with a wing box analysis and sensitivity capability, where in-plane loads determined by the wing box behavior serve as inputs to the panel aeroelastic behavior. Shape variations of the wing and its internal structure affect the panel both via its in-plane loads, and directly through the effects of its shape on its structural and aerodynamic matrices.

This work was limited to linear panel flutter using Piston Theory aerodynamics, and quasi-homogeneous composite construction. An effort to extend the work to cases of linear potential aerodynamics, active piezoelectric actuation, and non-linear structural and aerodynamic behavior is currently underway.

BIBLIOGRAPHY

1. Dowell, E.H., Aeroelasticity of Plates and Shells, Noordhoff International Publishers, Leyden, 1975.

2. Librescu, L., Elastostatics and Kinetics of Anisotropic and Heterogenous Shell Type Structures, Noordhoff International Publishers, Leyden, 1975.

3. Dugundji, J., "Theoretical Consideration of Panel Flutter at High Supersonic Mach Numbers", AIAA Journal, Vol. 4, No. 7, July 1966, pp. 1257-1266.

4. Eastep, F.E., and McIntosh, S.C., "Analysis of Nonlinear Panel Flutter and Response Under Random Excitation or Nonlinear Aerodynamic Loading", AIAA Journal, Vol. 9, No. 3, March 1971, pp. 411-418.

5. Sander, G., Bon, C., and Geradin, M., "Finite Element Analysis of Supersonic Panel Flutter", Internation Journal for Numerical Methods in Engineering, 7, pp. 379-394, 1973.

6. Yang, T.Y., "Flutter of Flat Finite Element Panels in Supersonic Unsteady Potential Flow", AIAA Journal, Vol. 13, No. 11, 1975, pp. 1502-1507.

7. Bismarck-Nasr, M.,N., "Finite Element Analysis of Aeroelasticity of Plates and Shells", ASME Applied Mechanics Reviews, Vol. 45, No. 12, pp. 461-482, December 1992.

8. Ibrahim, R.A., Orono, P.O., and Madaboosi, S.R., "Stochastic Flutter of a Panel Subjected to Random In Plane Forces, Part I: Two MOde Interaction", AIAA Journal, Vol. 28, No. 4, April 1990, pp. 694-702.

9. Liaw, D.G., "Supersonic Flutter of Laminated Thin Plates with Thermal Effects", Journal of Aircraft, Vol. 30, No. 1, Jan.-Feb. 1993, pp. 105-111.

10. Shore, C.P., "Flutter Design Charts for Biaxially Loaded Isotropic Panels", Journal of Aircraft, Vol. 7, No. 4, July-August 1970, pp. 325-329.

11. Lin, K.-J., Lu, P.-J., and Tarn, J.-Q., "Flutter Analysis of Composite Panels Using High Precision Finite Elements", Computers & Structures, Vol. 33, No. 2, pp. 561-574, 1989.

12. Chowdary, T.V.R., Parthan,S., and Sinha,P.K., "Finite Element Flutter Analysis of Laminated Composite Panels", Computers & Structures, Vol. 53, No. 2, pp. 245-251, 1994.

13. Shiau, L.-C., and Chang, J.-T., "Transverse Shear Effect on Flutter of Composite Panels", ASCE Journal of Aerospace Engineering, Vol. 5, No. 4, October 1992, pp. 465-479.

14. Lee, I., and Cho, M.-H., "Supersonic Flutter Analysis of Clamped Composite Panels Using Shear Deformable Finite Elements", AIAA Journal, Vol. 29, No. 5, May 1991, pp. 782-783.

15. Hajela, P., and Glowasky, R., "Application of Piezoelectric Elements in Supersonic Panel Flutter Suppression", AIAA Paper 91-3191, AIAA Aircraft Design Systems and Operations Meeting, Baltimore, MD, September 1991.

16. Scott, R.C., and Weishaar, T.A., "Controlling Panel Flutter Using Adaptive Materials", AIAA Paper 91-1007, April 1991.

17. Dowell, E.H., and Ilgamov, M., Studies in Nonlinear Aeroelasticity, Springer-Verlag, New York, 1988.

18. Sipcic, S.R., and Morino, L., "Dynamic Behavior of Fluttering Two-Dimensional Panels on an Airplane in Pull-Up Maneuver", AIAA Journal, Vol. 29, No. 8, pp. 1304-1312, August 1991.

19. Frampton, K.D., Clark, R.L., and Dowell, E.H., "State Space Modeling for Aeroelastic Panels Subject to Linearized Potential Flow Aerodynamic Loading", AIAA Paper 95-1294, Proceedings of the 36th AIAA/ASME/ASCE/AHS/ASC Structures, Structural Dynamics, and Materials Conference, New Orleans, LA, April 10-13, 1995, Vol. 2, pp. 1183-1189.

20. Durvasula, S., "Flutter of Simply Supported, Parallelogrammic, Flat Panels in Supersonic Flow", AIAA Journal, Vol. 5, No. 9, September 1967, pp. 1668-1673.

21. Kariappa, Somashekar, B.R., and Shah, C.G., "Discrete Element Approach to Flutter of Skew Panels with IN-Plane Forces Under Yawed Supersonic Flow", AIAA Journal, Vol. 8, No. 11, November 1970, pp. 2017-2022.

22. Srinivasan, R.S., and Babu, J.C., "Free Vibration and Flutter of Laminated Quadrilateral Plates", Computers & Structures, Vol. 27, No. 2, pp. 297-304, 1987.

23. Chowdary, T.V.R., Sinha, P.K., and Parthan, S., "Finite Element Flutter Analysis of Composite Skew Panels", Computers & Structures, Vol. 58, No. 3, pp. 613-620, 1996.

24. Haftka, R.T., and Gurdal, Z., Elements of Structural Optimization, Kluwer Academic Publishers, Dordrecht, Boston, London, Third Edition 1992 (Chapters 6,7)

25. Craig, R.R., "Optimization of a Supersonic Panel Subjected to a Flutter Constraint - A Finite Element Solution", AIAA Journal, March 1979, pp. 404-405.

26. Weisshaar, T.A., "Aeroelastic Optimization of a Panel in High Mach Number Supersonic Flow", Journal of Aircraft, Vol. 9, 1972, pp. 611-617.

27. Weisshaar, T.A., "Panel Flutter Optimization - A Refined Finite Element Approach" International Journal for Numerical Methods in Engineering, Vol. 10, pp. 77-91, 1976.

28. Van Keuren, G.M., and Eastep, F., "Use of Galerkin's Method for Minimum Weight Panels with Dynamic Constraints", Journal of Spacecraft and Rockets, Vol. 14, No. 7, July 1977.

29. Librescu, L., and Beiner, L., "Weight Mi nimization of Orthotropic Flat Panels Subjected to a Flutter Speed Constraint", AIAA Journal, Vol. 24, No. 6, June 1986, pp. 991-997.

30. Voss, H. M., and Dowell, E. H., "Effect of Aerodynamic Damping on Flutter of Thin Panels", AIAA Journal, Vol. 2, No. 1, January 1964, pp119-120.

31. Lottatti, I., "The Role of Damping on Supersonic Panel Flutter", AIAA Journal, Vol. 23, No. 10, October 1985, pp. 1640-1642.

32. Giles, G.L., "Equivalent Plate Analysis of Aircraft Wing Box Structures with General Planform Geometry", Journal of Aircraft, Vol. 23, No. 11, November 1986, pp. 859-864.

33. Giles, G.L., "Further Generalization of an Equivalent Plate Representation for Aircraft Structural Analysis", Journal of Aircraft, Vol. 26, No. 1, January 1989, pp. 67-74.

34. Livne, E., "Integrated Multidisciplinary Optimization of Actively Controlled Fiber Composite Wings", Ph.D. dissertation, Mechanical, Aerospace and Nuclear Engineering Department, University of California, Los Angeles, 1990.

35. Livne, E., "Analytical Sensitivities for Shape Optimization in Equivalent Plate Structural Wing Models", Journal of Aircraft, Vol. 31, No. 4, pp. 961-969, July-August 1994.

36. Livne, E., and Li, W-L., "Aeroservoelastic Aspects of Wing / Control Surface Planform Shape Optimization", AIAA Journal, Vol. 33, No. 2, February 1995, pp. 302-311.

37. Livne, E., and Milosavljevic, R., "Analytic Sensitivity and Approximation of Skin Buckling Constraints in Wing Shape Synthesis", Journal of Aircraft, Vol. 32, No. 5, September-October 1995, pp. 1102-1113.

38. Li, W-L., and Livne, E., "Analytic Sensitivities and Approximations in Supersonic and Subsonic Wing / Control Surface Unsteady Aerodynamics", AIAA Paper 95-1219, AIAA/ASME/ASCE/AHS/ASC 36th Structures, Structural Dynamics and Materials Conference, New Orleans, April 1995.

39. Haftka, R.T., and Gurdal, Z., "Elements of Structural Optimization", Third Edition, Kluwer Academic Publishers, Dordrecht, Boston, London 1991. (Chapter 6)

40. Pedersen, P., and Seyranian, A., "Sensitivity Analysis for Problems of Dynamic Stability", International Journal of Solids and Structures, Vol. 19, No. 4, pp. 315-335, 1983.

41. Seyranian, A., "Sensitivity Analysis of Multiple Eigenvalues", Mechanical Structures and Machines, Vol. 21, No. 2, pp. 261-284, 1993.

42. Golub, G., and Van Loan, C. F., Matrix Computations, 2nd edition, Johns Hopkins University Press, 1989.

43. Schmit, L.A., and Mehrinfar, M., "Multilevel Optimum Design of Structures with Fiber-Composite Stiffened-Panel Components", AIAA Journal, Vol. 20, Number 1, January 1982, pp. 138-147.

44. Schmit, L.A., and Ramanathan, R.K., "Multilevel Approach to Minimum Weight Design including Buckling Constraints", AIAA Journal, Vol. 16, No. 2, February 1978, pp. 97-104.

45. Starnes, J.H., Jr., and Haftka, R.T., "Preliminary Design of Composite Wings for Buckling, Stress and Displacement Constraints", Journal of Aircraft, Vol. 16, 1979, pp. 564-570.

46. Lecina, G., and Petiau, C., "Advances in Optimal Design with Composite Materials", in Computer Aided Optimal Design: Structuyral and Mechanical Systems, C.A. Mota Soares, editor, Springer Verlag, Berlin, 1987, pp. 943-953.

47. Ausman, J.D., Hangen, J.A., and Acevedo, D.A., "Application of a Local Panel Buckling Constraint within Automated Multidisciplinary Structural Analysis and Design", AIAA 92-1116, 1992 Aerospace Design Conference, February 3-6, 1992, Irvine, CA.

48. Ragon, S.A., Gurdal, Z., and Starnes Jr., J.H., "Optimization of Composite Box-Beam Structures Including The Effects of Subcomponent Interaction", AIAA 94-1410, Proceedings of the 35th AIAA/ASME/ASCE/AHS/ASC Structures, Structural Dynamics and Materials Conference, Hilton Kead, SC, April 18-20, 1994, pp. 818-828.

49. Bruhn, E.F., Analysis and Design of Flight Vehicle Structures, Tri State Offset Company, 1973, Chapter C5.

50. Antona, E., and Romeo, G., "Analytical and Experimental Investigation on Advanced Composite Wing Box Structures in Bending Including Effects of Initial Imperfections and Crushing Pressure", ICAS-86-4.2.3, 15th Congress of the International Council of the Aeronautical Sciences, London, England, September 1986, pp. 255-261.

51. Jones, R.M., Mechanics of Composite Materials, McGraw-Hill Book Company, New York 1975.

52. Whitney, J. M., Structural Analysis of Laminated Anisotropic Plates, Technomic Publishing Company, Lancaster, PA, 1987.

53. Vinson, J. R., and Sierakowski, R. L., The Behavior of Structures Composed of Composite Materials, Martinus Nijhoff Publishers, 1986.

54. Tsai, S.W., and Hahn, H.T., Introduction to Composite Materials, Technomic Publishing Company, Lancaster, PA, 1980.